Clinical Anatomy 00:00–00 (2016)

ORIGINAL COMMUNICATION

The Descending Branch of the Lateral Circumflex Femoral Artery As an Alternative Conduit for Coronary Artery Bypass Grafting: Experience From an Anatomical, Radiological and Histological Study

PETR LOSKOT,[1,2] ZBYNEK TONAR,[3]* JAN BAXA,[4] AND JIRI VALENTA[1]

[1]*Department of Anatomy, Faculty of Medicine in Pilsen, Charles University in Prague, Karlovarska 48, Pilsen, Czech Republic*
[2]*Department of Cardiac Surgery, University Hospital in Pilsen, Alej Svobody 80, Pilsen, Czech Republic*
[3]*Department of Histology and Embryology and Biomedical Center, Faculty of Medicine in Pilsen, Charles University in Prague, Karlovarska 48, Pilsen, Czech Republic*
[4]*Department of Imaging Methods and Biomedical Centre, Charles University and University Hospital in Pilsen, Alej Svobody 80, Pilsen, Czech Republic*

Introduction: The descending branch of the lateral circumflex femoral artery (DBLCFA) has been suggested as an option for use in coronary artery bypass grafting (CABG). Our aim was to combine radiological examination, surgical and anatomical preparation, and histological assessment of the DBLCFA to map its variability and to assess the benefits of this conduit in cardiac surgery. **Materials and Methods:** The pelvic and femoral arteries were examined by CT angiography (CTA) in 100 patients (aged 68.3 ± 9.3 years) to assess the variability of the DBLCFA. Anatomical dissections were performed on 20 cadavers. In 15 patients, an autologous DBLCFA was implanted during CABG. In 35 samples, possible atherosclerotic lesions were examined histologically. **Results:** The length of the potential DBLCFA conduits measured by CTA was 9.3 ± 2.9 cm, without correlating with the length of the thigh. Anatomical variations that would prevent the DBLCFA from being used in CABG were found in 27 out of 100 patients. Except for focal thickening of the intima, eccentric hypertrophy of the intima was found in three out of 35 samples. No inflammatory infiltration, foam cells, atheroma, or calcifications were found histologically. **Conclusions:** The DBLCFA is not to be used routinely or in preference to other grafts of choice. However, owing to its moderate variability, sufficient length, caliber, and rare atherosclerosis, it can be used in the absence of other suitable grafts as an alternative conduit implanted as a composite Y-graft end-to-side to the internal thoracic artery in patients without diabetic angiopathy, neuropathy or peripheral artery disease who are undergoing extensive or repeat coronary revascularization. Clin. Anat. 00:000–000, 2016.

*__Correspondence to__: Zbynek Tonar, Department of Histology and Embryology and Biomedical Centre, Faculty of Medicine in Pilsen, Charles University in Prague, Karlovarska 48, 301 66 Pilsen, Czech Republic. E-mail: zbynek.tonar@lfp.cuni.cz

Received 24 February 2016; Revised 30 April 2016; Accepted 4 May 2016

Published online in Wiley Online Library (wileyonlinelibrary.com). DOI: 10.1002/ca.22737

Key words: angiography; arteries; atherosclerosis; cardiovascular surgical procedure; coronary artery bypass grafting

INTRODUCTION

Arterial Grafts Routinely Used for CABG and Contraindications for Harvesting

From an anatomical point of view, an autologous arterial conduit should preferably be easily accessible and should have a diameter matching that of the target coronary vessels. The conduit should have a sufficient length available for harvesting with respect to bypassing the planned target vessels. The most commonly-used grafts are taken from the left internal thoracic artery (ITA) (Maddock et al., 2013; Koyama et al., 2014), followed by both left and right internal thoracic arteries. However, the ITA is not recommended and may be impossible to use in patients undergoing repeat cardiac surgery or with adhesions after lung or mediastinal surgery or radiotherapy of the mediastinum. The ITA is also not to be removed bilaterally from patients with expected difficulty in healing of the sternum, such as those suffering from diabetes, severe obesity, or osteoporosis (some of these contraindications may be relative). As shown by Pietrasik et al. (1999), bilateral ITA mobilization is possible only in patients with adequate diameter and length of the ITA common trunks and branches.

Another frequently-used conduit is the radial artery (RA) from the non-dominant forearm (Wendler et al., 2000). RA-multiple arterial coronary artery grafting (MABG) and ITA-MABG are therapies of choice in coronary artery bypass grafting (CABG) (Schwann et al., 2015), but the RA may not be removed in patients with a positive Allen's test, i.e., patients with insufficiency of the deep and superficial palmar arches anastomosing the radial and ulnar arteries, or with an unusual formation of the palmar arches (Tubbs and Loukas, 2006). Moreover, the RA may not be used when there is a history of trauma to the forearm and wrist or after partial thromboses following catheterization. The right gastro-epiploic artery is used preferentially in younger patients who are undergoing complete arterial revascularization (Hirose et al., 2002; Cho et al., 2011) of the right coronary artery and its branches (the right posterior interventricular branch, right posterolateral branch).

The Descending Branch of the Lateral Circumflex Femoral Artery

Most of the arterial conduits formerly proposed as alternative grafts have rarely been used in preference to the RA graft. However, owing to the increasing use of arterial conduits and the relative lack of suitable arterial conduits in patients undergoing repeat CABG, or with contraindications for harvesting the routinely-used conduits, alternative arterial grafts are still needed for such patients. Therefore, cardiac surgeons continue to search for new arterial grafts in order to avoid cardiac events associated with graft failure and to improve the life quality and expectancy of patients with coronary artery disease. The descending branch of the lateral circumflex femoral artery (DBLCFA) has been suggested and tested in Japan by Tatsumi et al. (1996) as an option for use in CABG. Fabbrocini et al. (2003) reported excellent clinical results and mid-term patency rates. However, the data on variability and practical use remain controversial. Yamashita et al. (2005) found that only 68.6% of 70 patients had a DBLCFA suitable for bypass because the remainder had wall irregularities, stenosis or hypoplasia.

On rare occasions, the lateral circumflex femoral artery (LCFA) can be used as an interposition graft (Anderson et al., 2004). Radiological studies on the DBLCFA showed that it seems relatively spared from atherosclerosis (Halvorson et al., 2008). Whereas the branching patterns of the circumflex femoral arteries have been thoroughly mapped by Vazquez et al. (2007) and the clinical anatomy of the medial femoral artery has been reported in detail by Clarke and Colborn (1993), the variability and clinical anatomy of the DBLCFA itself are mostly unknown and only exceptional case studies have been reported (Goel et al., 2015). Despite being used successfully as the pedicle of anterolateral thigh flaps or fibular grafts in plastic and reconstructive surgery and orthopedics (Choi et al., 2014; Gokhan et al., 2014; Jia et al., 2015), the DBLCFA is still extremely rarely used for CABG. Despite preliminary studies on its preparation (Loskot et al., 2014), anatomical and histological studies linked with angiographic assessment of atherosclerosis in patients undergoing CABG are still lacking, and this became the rationale for the present study.

The aim of this study was to combine radiological examination, surgical and anatomical preparation, and histological assessment of the DBLCFA to map its variability and to assess the benefits and limitations of this conduit in cardiac surgery.

PATIENTS AND METHODS

CT Angiography (CTA)

To assess the variability of the DBLCFA, CTA data from 100 patients examined at the Department of Imaging Methods, Charles University and University Hospital in Pilsen were used. The patients (80 males, 20 females, mean age $\pm$SD 68.3 ± 9.3 years) were indicated for CTA of the abdominal aorta and peripheral arteries with suspicion of peripheral arterial disease. All of the patients gave informed consent and the study accorded with the rules of the Ethics Committee of the University Hospital and Faculty of Medicine in Pilsen, Charles University in Prague. The

TABLE 1. Body Height, Body Mass Index (BMI), Length of the Thigh, and Length of the Descending Branch of the Lateral Circumflex Femoral Artery (DBLCFA) in Patients ($n = 100$) Undergoing Pelvic and Femoral CT Angiography

	Body height (cm)	BMI	Length of the thigh (cm)	Length of the DBLCFA (cm)
Mean (± SD)	171.8	28.1	46.2 (±3.3)	9.3 (±2.9)
Value range	150–197	19.1–27.2	38.6–54.5	2.1–17.4

In nine patients (9%), the diameter of the whole DBLCFA was <2 mm and these patients were excluded from further measurements. The length of the thigh was measured as the distance between the anterior superior iliac spine and the upper border of the patella. The length of the DBLCFA was measured from the origin of the artery to its branching in the muscle or up to the 2 mm diameter in the periphery. The range denotes the minimum and maximum values in the patients included in the study.

Somatom Definition Flash (Siemens Healthcare, Erlangen, Germany) CTA was used with a collimation of 128 × 0.6 mm. The DBLCFA in the left limb was measured in detail in 91 of the patients, and the DBLCFA on the right or both sides was measured in the other nine. The left limb was preferred in view of the usual positioning of the patient during graft harvesting at the operating theatres of the Department of Cardiac Surgery, University Hospital in Pilsen (this might differ among hospitals and surgery teams). The length of the DBLCFA was measured from its origin to its branching in the muscle or up to the 2 mm diameter in the periphery.

Anatomically significant stenoses (reduction of >50% of the original lumen diameter) were tracked and the lesions were classified using a semiquantitative scale: 0 (no lesion), 1 (initial lesion), 2 (minor calcifications without distinct stenosis), 3 (clearly visible atherosclerotic lesion with stenosis <50%), and 4 (atherosclerotic lesions with a significant stenosis >50%). CTA settings, image processing and scoring were compatible with the study by Kristanto et al. (2012).

Anatomical Dissection of the DBLCFA

The DBLCFA was dissected in 20 cadavers (13 males, seven females, mean age ± SD 63.4 ± 14.7 years) donated according to the Czech law within the Body donor programme to the Department of Anatomy, Faculty of Medicine in Pilsen, Charles University in Prague, for educational and scientific purposes. Only cadavers with no history of ischemic limb disease were included in the study. The cadavers were used for training in dissection and for exploring possible modifications of the graft harvesting. From the proximal and the middle portions of each DBLCFA, approximately 4 mm-long segments were removed for histological examination.

Conduits Used in CABG

In 15 patients (14 males, one female, mean age ± SD 66.9 ± 6.5 years) undergoing CABG at the Department of Cardiac Surgery, University Hospital in Pilsen, the DBLCFA was used for revascularization surgery. All patients selected for the study were undergoing first-

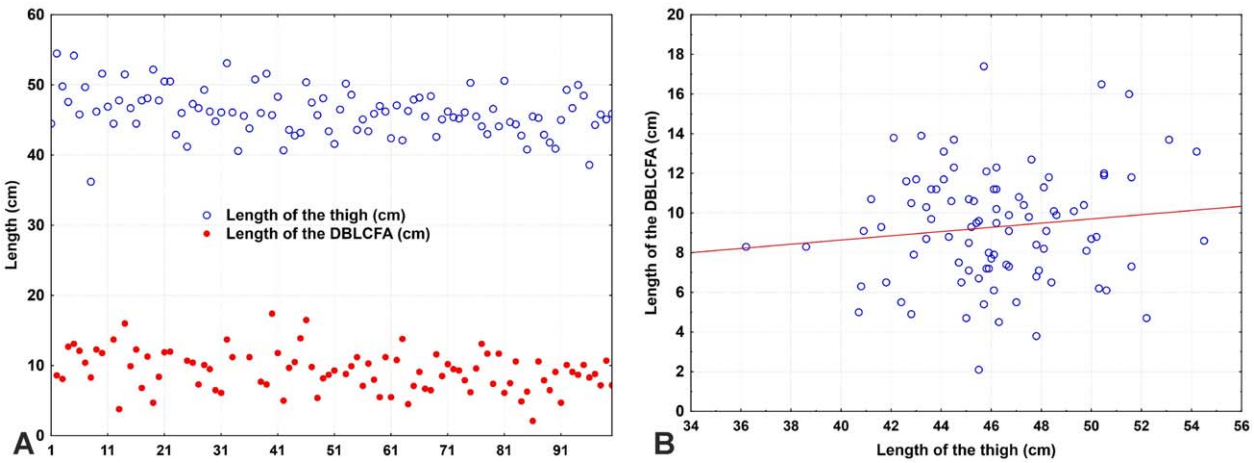

Fig. 1. Length of the thigh and length of the descending branch of the lateral circumflex femoral artery (DBLCFA) in patients undergoing pelvic and femoral CT angiography. **A**—Case profiles of the patients under study. **B**—The length of the thigh did not correlate with the length of the DBLCFA (Pearson coefficient 0.12, non-significant linear fitting (red line) with $P = 0.24$). See Table 1 for a summary of the data. [Color figure can be viewed in the online issue, which is available at wileyonlinelibrary.com.]

TABLE 2. Morphological Variability of the DBLCFA in Patients ($n = 100$) Undergoing Pelvic and Femoral CT Angiography

Hypoplastic DBLCFA (very thin lumen, insignificant circulation)	Gracile DBLCFA (involved in local circulation, but with diameter <2 mm at the origin)	DBLCFA originating from the superficial artery of the thigh	DBLCFA originating from the deep artery of the thigh	Early proximal DBLCFA bifurcation or more muscular branches	DBLCFA as a part of collateral circulation
Eight cases	One case	Four cases	Two cases	Two cases	Six cases (one case in obliterated superficial artery of the thigh)

time CABG, but they lacked conduits from traditional sources for complete arterial revascularization. All patients signed the informed consent for the procedure. From the proximal and distal ends of each DBLCFA, approximately 4 mm-long surplus segments were removed for histological examination. The DBLCFA conduits were implanted to the left-sided ITA as Y-grafts to bridge either the lateral branch of the anterior interventricular branch or the left marginal branch of the circumflex branch. During a three month follow-up, CTA was performed to assess graft patency.

Histology of the DBLCFA

Vascular segments of the DBLCFA removed either during the anatomical dissections or prior to conduit implantation (CABG) were fixed in buffered formalin. At least 12 histological sections per sample were cut perpendicularly to the longitudinal axis of the artery. Vessel morphology was examined using hematoxylin-eosin staining and a combination of Verhoeff's hematoxylin and green trichrome. Any findings of atherosclerotic lesions were classified according to Stary et al. (1994).

RESULTS

CT Angiography of the DBLCFA

The measurements of the DBLCFA are summarized in Table 1 together with basic information about the patients enrolled in the study. In nine patients (9%), the diameter of the whole DBLCFA was <2 mm. These

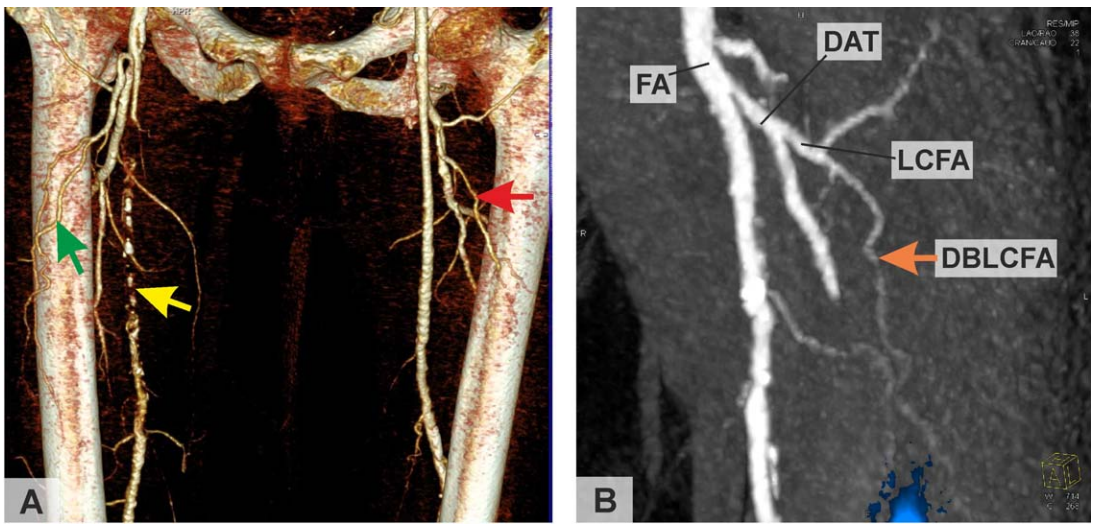

Fig. 2. The descending branch of the lateral circumflex femoral artery (DBLCFA) as a part of the collateral circulation and as a gracile variant in patients ($n = 100$) undergoing pelvic and femoral CT angiography. **A**—In six patients, the DBLCFA was a part of the collateral circulation (on the patient's right side, green arrow) because of stenosis of the superficial femoral artery (yellow arrow). **B**—In one patient, the diameter of the proximal DBLCFA (orange arrow) was below <2 mm, which was counted as a gracile variant ineligible as a CABG conduit. The branching pattern is followed from the femoral artery (FA), deep artery of thigh (DAT), and lateral circumflex femoral artery (LFCA) to the DBLFCA. [Color figure can be viewed in the online issue, which is available at wileyonlinelibrary.com.]

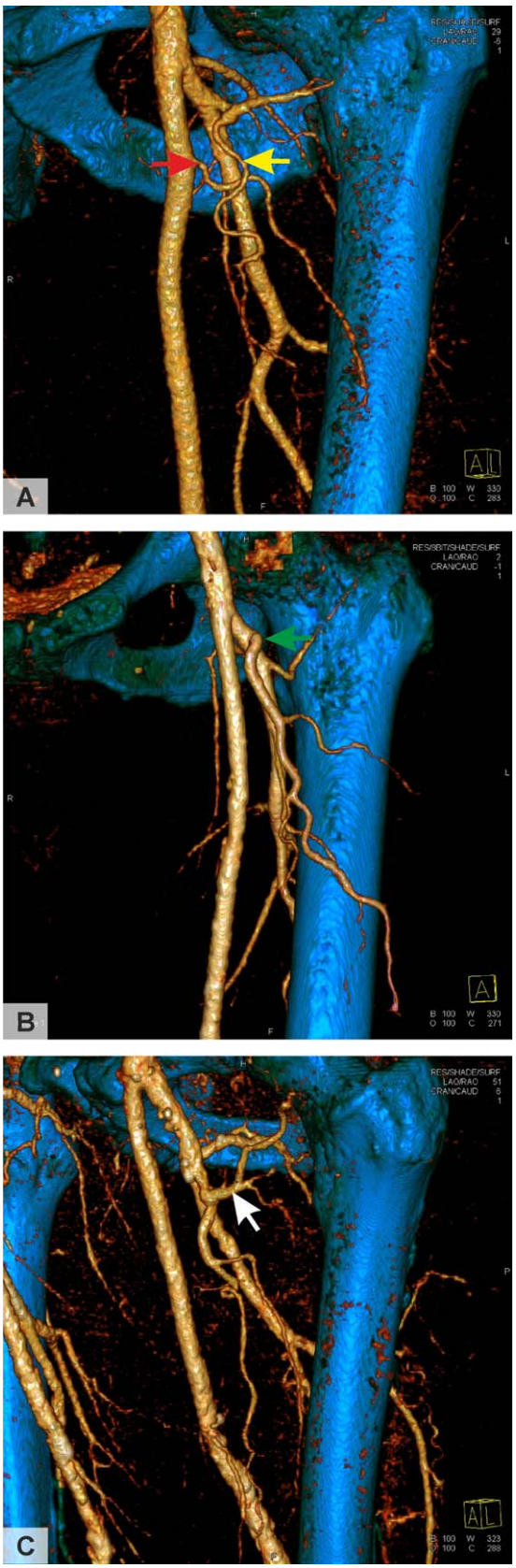

patients were excluded from further measurements because the diameter was insufficient for potential conduit harvesting. The minimum length of the potential DBLCFA conduit with diameter $>$ 2.0 mm was 2.1 cm and the maximum was 17.4 cm. Most of the findings were close to the mean value of 9.3 cm, with a standard deviation of 2.9 cm (see Fig. 1A for a graphical plot of all the cases). The mean diameter of the DBLCFA at its origin was 2.9 mm (2.1–3.4 mm). The length of the DBLCFA was not correlated with the length of the thigh (Pearson correlation coefficient 0.12, $P > 0.24$, Fig. 1B). The morphological variability among the 100 patients is summarized in Table 2 and these findings are illustrated in Figures (2 and 3). The occurrences of stenoses ($>$50%) and atherosclerotic lesions are summarized in Table 3.

Surgical and Anatomical Dissection of the DBLCFA

On the basis of our experience, the recommended preparation of the DBLCFA for CABG is as follows: The procedure starts with a 10–15 cm long anterolateral section in an axis connecting the anterior superior iliac spine with the middle of the patella. The incision (Fig. 4A) originates at the level of the lower margin of the inguinal ligament. The fascia lata is cut anteriorly to the iliotibial tract, but without damaging the fascia of the tensor fasciae latae muscle. After penetrating between the fasciae of the rectus femoris and vastus lateralis muscles using a blunt dissection technique, we approach the surface of the vastus intermedius muscle. The DBLCFA is found on its surface, accompanied by the muscular branches of the femoral nerve. This is to be separated from the DBLCFA to prevent injury to those femoral nerve branches. On the proximal end of the conduit, the DBLCFA is ligated approximately 1–2 cm distal to its origin from the LCFA. The ascending branch of the LCFA is to be protected because it contributes to the vascular supply to the hip joint. The distal end of the DBLCFA is tracked and ligated either before the DBLCFA enters the vastus intermedius or before it splits into the minor muscular branches. Any major branches of the DBLCFA are ligated as well. Using a harmonic scalpel, the DBLCFA is removed together with the accompanying veins (usually two of them) that share the same tunica adventitia connective tissue with the artery. Any

Fig. 3. Variability of the descending branch of the lateral circumflex femoral artery (DBLCFA) in patients ($n = 100$) undergoing pelvic and femoral CT angiography. **A**—Duplication of the DBLCFA. In addition to the regular DBLCFA (yellow arrow), another artery supplies the same region but originates from the femoral artery (red arrow). **B**—In two patients, very early branching of the DBLCFA (green arrow) would make the artery ineligible as a CABG conduit. **C -** In one patient, a conspicuous transverse muscular branch (white arrow) of the DBLCFA was found. [Color figure can be viewed in the online issue, which is available at wileyonlinelibrary.com.]

TABLE 3. Occurrence of Stenosis and Atherosclerotic Lesions Between the Aorta, the Common Femoral Artery, the Deep Artery of the Thigh, and the Superficial Artery of the Thigh in Patients ($n = 100$) Undergoing Pelvic and Femoral CT Angiography

Significant stenosis (>50%) of the deep artery of thigh	Significant stenosis (>50%) of the superficial artery of thigh	Significant stenosis (>50%) between the aorta and the common femoral artery	Significant stenosis (>50%) in either the pelvic or femoral arteries	Significant atherosclerosis (grade 3-4) of the DBLCFA
Two cases	50 cases	50 cases	72 cases	19 cases

Significant stenoses (>50% of the original lumen diameter) between the aorta, the common femoral artery, the deep artery of the thigh, and the superficial artery of the thigh were tracked and marked. Atherosclerotic lesions were classified using a semiquantitative scale: 0 (no lesion), 1 (initial lesion), 2 (minor calcifications without distinct stenosis), 3 (clearly visible atherosclerotic lesion with stenosis <50%), and 4 (atherosclerotic lesions with a significant stenosis >50%).
Abbreviations used: CABG, coronary artery bypass grafting; CTA, CT angiography; DBLCFA, descending branch of the lateral circumflex femoral artery; ITA, internal thoracic artery; LCFA, lateral circumflex femoral artery; MABG, multiple arterial coronary artery grafting; RA, radial artery.

unnecessary mechanical contacts with the DBLCFA are to be avoided to prevent its spasm (no-touch technique published by Souza et al., 2002). To prevent vascular spasm, the DBLFCA is to be dilated by instillation of isotonic saline solution, vasodilator, or heparinized blood. Excess pressure should be avoided to prevent intramural edema. The proximal and distal ends of the conduit are marked. All separate anatomical layers of the wound are closed. If any coagulopathy is anticipated, or if the patient has been treated with anticoagulants or antiplatelet drugs, postoperative Redon drainage is applied. After the surgery, the limb can be wrapped with an elastic bandage. The time required for the conduit preparation and harvesting averaged between 15 and 25 min. An example of the DBLCFA conduit implanted as a Y-graft to the left ITA during the CABG is shown in Figure 4B. During follow-up, there were no postoperative complications such as vascular supply or innervation disorders, difficulty in healing, infection, edema, or major hematoma.

Histology of the DBLCFA

In 15 of the 20 samples of DBLCFA examined from cadavers and in 13 of the 15 samples taken from the surplus ends of CABG conduits, no atherosclerotic lesions were found. The arteries were surrounded with a rich adventitia connective tissue (Fig. 5A-C), which also contained the vasa vasorum (Fig. 5A) and the nervi vasorum (Fig. 5B). The wall thickness was in the range 340–500 μm. In eight samples there was focal thickening of the intima (Fig. 5D). In three of these, eccentric hypertrophy of the intima was observed (Fig. 5E). Most of the samples (Fig. 5F) had a normal intima thickness with no signs of proliferation or inflammatory infiltration. The internal elastic lamina was well preserved (Fig. 5F). No foam cells, fibrous cap-covered atheroma, neovascularization, inflammatory infiltration, calcification, or other signs of vulnerable atherosclerotic lesions were found in any of the DBLCFA samples included in this study.

DISCUSSION

Anatomical Study Implications and Recommendations for the Use of DBLCFA In CABG

Before harvesting, it should be determined whether the DBLCFA is necessary for collateral circulation when there is stenosis of the surrounding arteries of the thigh. A thorough mapping of collateral pathways in peripheral arterial disease was provided by Wooten et al. (2014) and recently commented on by Anwar and Aydin (2015). The DBLCFA is a common route for collateralization in the presence of femoropopliteal occlusive disease, which may preclude its harvesting. Hage and Woerdeman (2004) reported a patient with partial necrosis of the foot and calf caused by interruption of the DBLCFA, which served as a critical collateral for the obstructed superficial femoral artery. Interestingly, the experience of Sakakibara et al. (1999) suggested that larger caliber DBLCFAs could be of greater importance as collateral channels and therefore should be rather saved and not harvested. Moreover, Gaiotto et al. (2013) found a high patency rate and positive luminal adaptation when they used the DBLCFA in 32 patients with CABG, but owing to a high incidence of anatomical variations they suggested that preoperative femoral angiographic examination was mandatory. However, this would be difficult in patients suffering from overall atherosclerosis, which often entails deterioration of kidney function, and patients with severe kidney problems may be unsuited for CTA. These controversial findings show that to date there has been no uniform strategy for harvesting the DBLCFA. Our CTA results contribute to the debate by revealing anatomical variations that would prevent the DBLCFA from being used for CABG in 27 out of 100 patients. These results suggest that even in patients unsuitable for preoperative CTA, the morphology of the DBLCFA is worth exploring whenever alternative arterial grafts are sought, where the first choice grafts (ITA and RA) are not available. We speculate that some of the inconsistent results concerning variability could be partially explained by

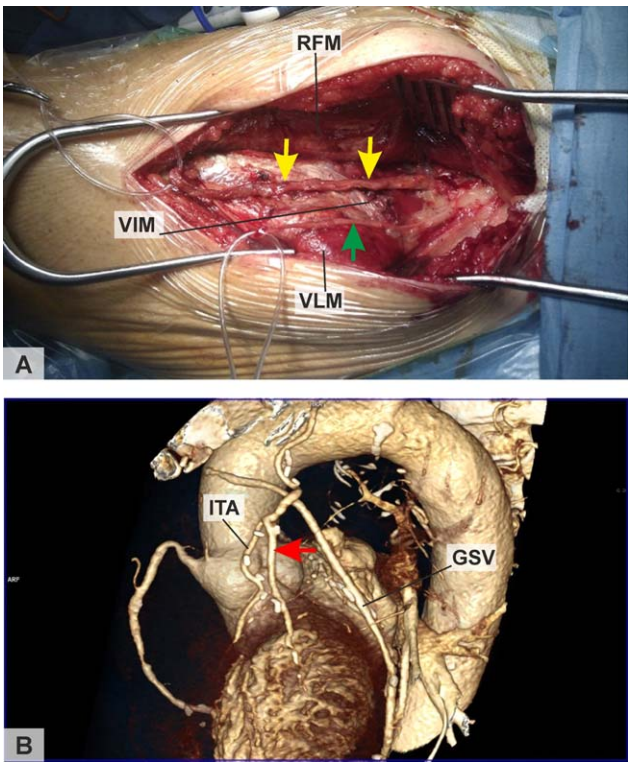

Fig. 4. Dissection of the DBLCFA prior to coronary artery bypass grafting (CABG) and an example of a DBLCFA conduit used for CABG. **A**—Left thigh with an incision within an axis connecting the anterior superior iliac spine with the middle of the patella. After penetrating between the fasciae of the rectus femoris (RFM) and vastus lateralis (VLM) muscles, the DBLCFA (yellow arrows) with accompanying veins is found lying on the surface of the vastus intermedius muscle (VIM). The muscular branches of the femoral nerve (green arrow) are prepared laterally to the DBLCFA. **B**—CT angiography reconstruction showing an example of a DBLCFA conduit (red arrow) implanted as a Y-graft to the left internal thoracic artery (ITA) during a CABG. Additionally, a graft from the great saphenous vein (GSV) implanted to the aorta is shown. In this particular patient, the diagonal branch of the anterior interventricular branch was especially well developed, thus supplying a substantial mass of myocardium. Because of that and of the patient's age (<50 years), we preferred to use an arterial graft for this position. Selective coronarography showed that the left marginal artery was a chronically obliterated vessel weakly filled with contrast medium and some minor calcifications, so the revascularization was partially questionable. In view of the age and history of the patient, the final decision was to perform the bypass also using the GSV. [Color figure can be viewed in the online issue, which is available at wileyonlinelibrary.com.]

differences among populations from different countries in which the research on DBLCFA variability was conducted, but no such comparison has been published so far.

Practical Recommendations

Routinely, there must be no claudication or decreased peripheral pulse on the popliteal, posterior tibial, or dorsalis pedis arteries before DBLCFA harvesting. CTA seems to be an ideal non-invasive method for preoperative assessment of the condition and diameters of the DBLCFA. Therefore we suggest that a typical patient who would benefit from DBLCFA grafting is relatively young, with total arterial or repeated extensive arterial coronary revascularization. However, in patients suffering from peripheral arterial disease, a previously performed CTA could be reassessed for the condition of the DBLCFA.

Histological examination demonstrated the absence of or a very low prevalence of atherosclerotic lesions, none of which were advanced or even vulnerable (Fleiner et al., 2004). This proneness to atherosclerosis even in patients undergoing coronary revascularization surgery seems to be similar to that described for the ITA (Sisto and Isola, 1989; Wharton et al., 1994). We found no comparable published papers on histological analysis of the DBLCFA. However, the DBLCFA is a muscular limb artery classified as a spastic type III according to He (1999, 2013). This suggests that a higher incidence of spasm might be expected than in somatic or splanchnic arteries.

Contractility, Functional and Clinical Classification of DBLCFA and Other Arterial Grafts

Histological and physiological studies revealed considerable differences in microscopic anatomy and contractility among various arterial conduits. This is of great importance because vasospasm is supposed to be the extreme form of vasoconstriction, which can be caused by physical or pharmacological stimuli (spasmogens). Mechanical stimulation is minimized during surgery by using the "no-touch" technique described above. According to He et al. (1995), type I spasmogens such as endothelin, prostanoids and α1-adrenoreceptor agonists strongly contract arterial grafts even when the endothelium is intact. Type II spasmogens such as serotonin induce only weak vasoconstriction in arteries with intact endothelium. However, the effect of type II spasmogens is greatly enhanced when the endothelium is injured during surgical handling.

According to their anatomical structure and reaction to vasoconstrictors, He (1999) introduced a functional classification of arterial grafts: (i) Type I are somatic and less spastic arteries such as the ITA and inferior epigastric artery, the ITA being more elastic than all other grafts (van Son et al., 1990; He, 2013); (ii) Type II comprises splanchnic arteries with a greater incidence of spasm such as the gastro-epiploic or splenic artery; (iii) Type III comprises muscular limb arteries prone to spasm such as the RA, ulnar artery or LCFA. Our histological findings support the morphological background of this classification because the DBLCFA samples under study contained only internal elastic laminae at the intima-media

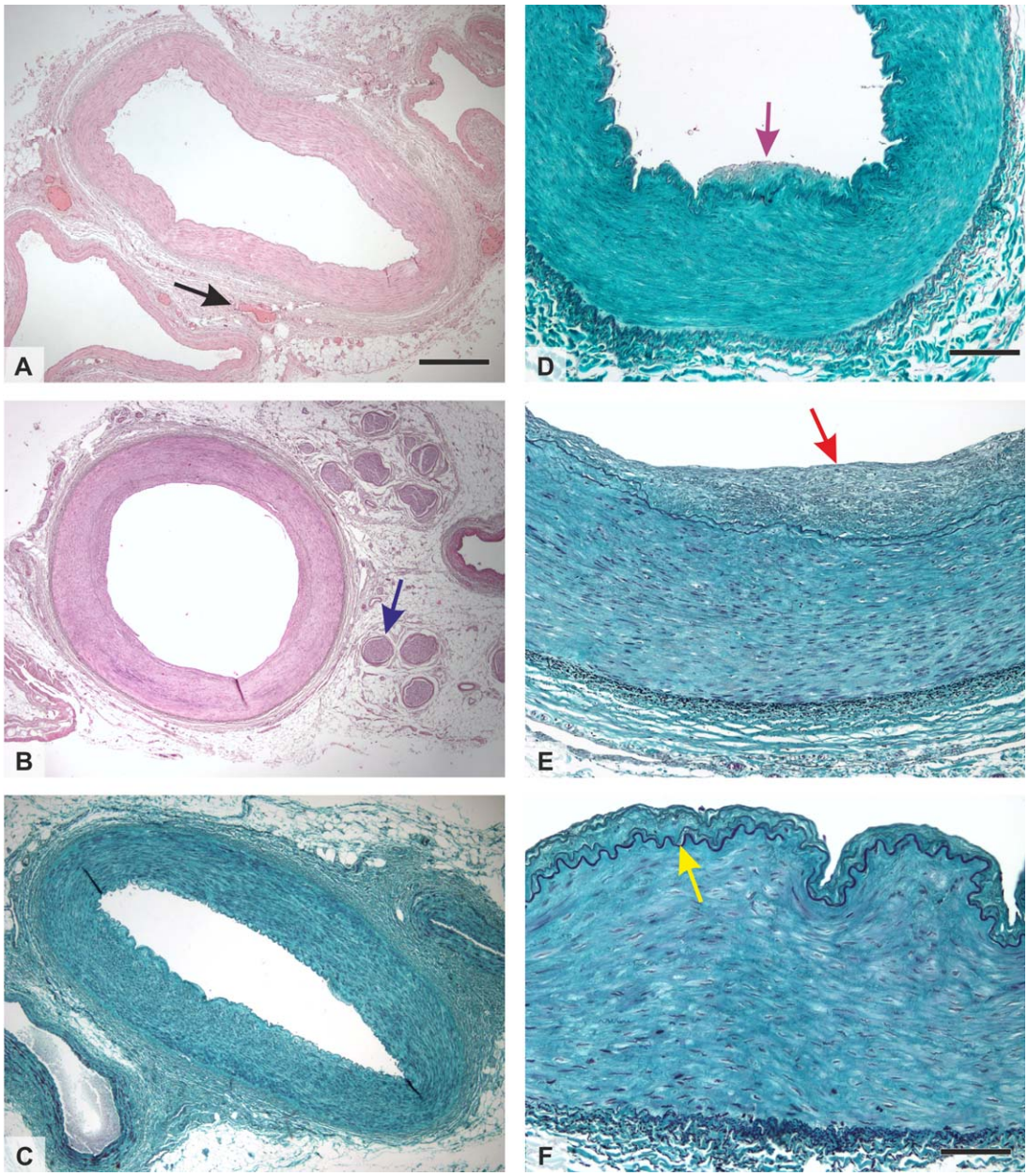

Fig. 5. Histological findings in the descending branch of the lateral circumflex femoral artery. Samples were taken from the proximal and distal ends of grafts of sufficient length. The arteries were surrounded by a rich adventitia connective tissue (A–C), which also contained the vasa vasorum (A, black arrow) and the nervi vasorum (B, blue arrow). Most of the samples had no histological signs of atherosclerosis. No atheroma, inflammatory infiltration, neovascularization or calcifications were found. In several samples there was focal thickening of the intima (D, purple arrow). In three samples, eccentric hypertrophy of the intima was observed (E, red arrow). Most of the samples (F) had a normal intima thickness with no signs of proliferation or inflammatory infiltration. The internal elastic lamina was well preserved (F, yellow arrow), thus delineating the border between the tunica media and the tunica intima layers. All samples under study were typical muscular arteries with no elastic lamellae within the tunica media layer. Hematoxylin-eosin stain (A–B) and Verhoeff's hematoxylin with green trichrome stain (D–F). Scale bars 500 μm (A–C), 200 μm (D–E), 100 μm (F). [Color figure can be viewed in the online issue, which is available at wileyonlinelibrary.com.]

border and few outer elastic laminae at the media-adventitia border.

Moreover, there are considerable differences in endothelial function among arterial grafts. The endothelium in the ITA releases more NO than in the RA, and the ITA also shows a more pronounced endothelium-dependent smooth muscle relaxation than most other arterial grafts (He, 2013; He and Taggart, 2016). The superior endothelial function of the ITA probably contributes to its excellent long-term patency.

Study Limitations

Our study was not intended to produce data on long-term patency of the grafts, but sufficient data on this topic have already been published by Fabbrocini et al. (2003). Although the groups of patients in our study had a similar mean age, as did the cadavers used for dissections, the patients in the CTA part of our study had a relatively high prevalence of stenoses between the aorta and the common femoral artery and within the DBLCFA, far exceeding the prevalence of atherosclerosis in patients undergoing CABG or in samples taken from the cadavers. This inconsistency arose because the CTA was a medical procedure indicated in patients for whom ischemic limb disease needed to be assessed. Therefore, these patients were not a representative sample of a general population and there could have been a gender bias. While the anatomical variability found in these patients could be used as a good estimate, the occurrence of stenosis and atherosclerosis was most likely biased in comparison with a general population of the same age. Another limitation is that the study only deals with morphology and provides no data on the endothelial function or pharmacological properties of the DBLCFA samples. The histological part of the study assessed atherosclerosis only in 4 mm-long segments taken from the DBLCFA, so we cannot exclude the possibility that the incidence of discrete atherosclerotic lesions was underestimated. Moreover, the cadavers were pre-selected to avoid any known ischemic limb disease.

In conclusion, this study combined CT angiography, surgical preparation, and anatomical and histological assessment of the descending branch of the lateral circumflex artery. The artery showed moderate anatomical variability and, in 32 out of 35 cases, no advanced atherosclerosis except for intima thickening. We provided a description of the surgical preparation of the DBLCFA conduit for relatively safe and fast harvesting. In view of their typical length, diameter, and caliber, DBLCFA conduits are comparable to those of the gastro-epiploic artery and therefore predetermined to be implanted end-to-side to the left-sided ITA as a composite Y-graft to bridge either the lateral branch of the anterior interventricular branch or the left marginal branch of the circumflex branch in a selected group of patients. The DBLCFA is not to be used routinely or in preference to other grafts of choice; despite promising mid-term patency results, long-term patency is unknown. The DBLCFA is not universally usable as it was not available in 27% of the patients and requires CTA beforehand. The graft might be inappropriate for use in a high percentage of patients (19%) owing to anatomical variations such as short length, narrow lumen diameter, and silent atherosclerosis (Gaiotto et al., 2013). Another drawback is that the DBLCFA is a muscular limb artery classified as more prone to vasospasm because of its greater sensitivity to circulating catecholamines and other vasoconstrictors than more elastic conduits (e.g. the ITA).

The DBLCFA can currently be recommended as a graft in CABG only in the rare circumstance that no other arterial or venous graft material is available, and only if there is sufficient institutional experience and skill to avoid any risks to the muscular branches of the femoral nerve and the vascular supply to the hip. However, the DBLCFA can be recommended for further testing for use as an alternative arterial conduit for complete or extensive coronary revascularization (Windecker et al., 2014) in carefully-selected patients without diabetic angiopathy, neuropathy, or peripheral arterial disease.

ACKNOWLEDGMENTS

The authors hold the greatest respect for those who donated their bodies to our anatomy course within the Body Donor Program. They are grateful to those individuals for giving us the opportunity to further our knowledge of the human body. The donors of bodies used in this study were also honored during our annual memorial service. This study was supported by the Prvouk P36 Project of the Charles University in Prague and by the National Sustainability Program I (NPU I) Nr. LO1503 provided by the Ministry of Education, Youth and Sports of the Czech Republic. This study was also partially supported by the Ministry of Health of the Czech Republic, Project Nr. AZV 15-32727A.

REFERENCES

Anderson CA, Filsoufi F, Kadner A, Adams DH. 2004. Repair of a left main coronary artery aneurysm using the circumflex femoral artery as a Y-interposition graft. Ann ThoracSurg 78:314–316.

Anwar MO, Aydin A. 2015. The significance of the pelvic collateral circulation in aorto-iliac disease. ClinAnat 28:558–559.

Cho KR, Hwang HY, Kim JS, Kim KB. 2011. Right gastroepiploic artery graft for myocardial revascularization: prevalence of atherosclerosis and availability as a conduit. Ann ThoracSurg 91: 440–443.

Choi HJ, Jung KH, Wee SY. 2014. Clinical analysis of risk factors of the patency of the descending branch of the lateral circumflex femoral artery. J PlastSurg Hand Surg 48:396–401.

Clarke SM, Colborn GL. 1993. The medial femoral circumflex artery: Its clinical anatomy and nomenclature. ClinAnat 6:94–105.

Fabbrocini M, Fattouch K, Camporini G, DeMicheli G, Bertucci C, Cioffi P, Mercogliano D. 2003. The descending branch of lateral femoral circumflex artery in arterial CABG: Early and midterm results. Ann Thorac Surg 75:1836–1341.

Fleiner M, Kummer M, Mirlacher M, Sauter G, Cathomas G, Krapf R, Biedermann BC. 2004. Arterial neovascularization and inflammation in vulnerable patients: early and late signs of symptomatic atherosclerosis. Circulation 110:2843–2850.

Gaiotto FA, Vianna CB, Busnardo FF, Parga JR, Dallan LA, Cesar LA, Stolf NA, Jatene FB. 2013. The descending branch of the lateral femoral circumflex artery is a good option in CABG with arterial grafts. Rev Bras Cir Cardiovasc 28:317–324.

Goel S, Arora J, Mehta V, Sharma M, Suri RK, Rath G. 2015. Unusual disposition of lateral circumflex femoral artery: Anatomical description and clinical implications. World J Clin Cases 3:85–88.

Gokhan M, Ulusal AE, Atik A, Sargin S, Ulusal B, SukruSahin M. 2014. Descending branch of the lateral circumflex femoral artery as a recipient vessel for vascularized fibular grafts. Microsurgery 34:633–637.

Hage JJ, Woerdeman LA. 2004. Lower limb necrosis after use of the anterolateral thigh free flap: is preoperative angiography indicated? Ann PlastSurg 52:315–318.

Halvorson EG, Taylor HO, Orgill DP. 2008. Patency of the descending branch of the lateral circumflex femoral artery in patients with vascular disease. PlastReconstrSurg 121:121–129.

He GW. 1999. Arterial grafts for coronary artery bypass grafting: biological characteristics, functional classification, and clinical choice. Ann ThoracSurg 67:277–284.

He GW. 2013. Arterial grafts: clinical classification and pharmacological management. Ann CardiothoracSurg 2:507–518.

He GW, Taggart DP. 2016. Spasm in arterial grafts in coronary artery bypass grafting surgery. Ann ThoracSurg 101:1222–1229.

He GW, Yang CQ, Starr A. 1995. Overview of the nature of vasoconstriction in arterial grafts for coronary operations. Ann ThoracSurg 59:676–683.

Hirose H, Amano A, Takanashi S, Takahashi A. 2002. Coronary artery bypass grafting using the gastroepiploic artery in 1,000 patients. Ann ThoracSurg 73:1371–1379.

Jia YC, Chen HH, Kang QL, Chai YM. 2015. Combined Anterolateral Thigh and Anteromedial Thigh Flap for Extensive Extremity Reconstruction: Vascular Anatomy and Clinical Application. J ReconstrMicrosurg In Press, doi: 10.1055/s-0035-1558985.

Kristanto W, van Ooijen PM, Groen JM, Vliegenthart R, Oudkerk M. 2012. Small calcified coronary atherosclerotic plaque simulation model: minimal size and attenuation detectable by 64-MDCT and MicroCT. Int J Cardiovasc Imaging 28:843–853.

Koyama S, Itatani K, Yamamoto T, Miyazaki S, Kitamura T, Taketani T, Ono M, Miyaji K. 2014. Optimal bypass graft design for left anterior descending and diagonal territory in multivessel coronary disease. InteractCardiovascThoracSurg 19:406–413.

Loskot P, Baxa J, Hajek T, Valenta J. 2014. A study of the morphology of the descending branch of the lateral circumflex femoral artery (DBLCFA) as a possible vascular graft for the reconstruction of coronary arteries using angio CT. RozhlChir 93:307–310.

Maddock S, Tang GHL, Aronow WS, Malekan R. 2013.Total Arterial Revascularization in Coronary Artery Bypass Grafting Surgery. In: Aronow WS, editor. Artery Bypass. Rijeka: InTech. p 119–133.

Pietrasik K, Bakon L, Zdunek P, Wojda-Gradowska U, Dobosz P, Kolesnik A. 1999. Clinical anatomy of internal thoracic artery branches. ClinAnat 12:307–314.

Sakakibara Y, Abe M, Hiramatsu Y, Shigeta O, Ishikawa S, Jikuya T, Mitsui T. 1999. The descending branch of the lateral femoral circumflex artery for coronary artery bypass grafting. J ThoracCardiovascSurg 118:753–754.

Schwann TA, Hashim SW, Badour S, Obeid M, Engoren M, Tranbaugh RF, Bonnell MR, Habib RH. 2015. Equipoise between radial artery and right internal thoracic artery as the second arterial conduit in left internal thoracic artery-based coronary artery bypass graft surgery: a multi-institutional study. Eur J CardiothoracSurg pii: ezv093.

Sisto T, Isola J. 1989. Incidence of atherosclerosis in the internal mammary artery. Ann ThoracSurg 47:884–886.

Souza DS, Dashwood MR, Tsui JC, Filbey D, Bodin L, Johansson B, Borowiec J. 2002. Improved patency in vein grafts harvested with surrounding tissue: results of a randomized study using three harvesting techniques. Ann ThoracSurg 73:1189–1195.

Stary HC, Chandler AB, Glagov S, Guyton JR, Insull W, Jr, Rosenfeld ME, Schaffer SA, Schwartz CJ, Wagner WD, Wissler RW. 1994. A definition of initial, fatty streak, and intermediate lesions of atherosclerosis. A report from the Committee on Vascular Lesions of the Council on Arteriosclerosis, American Heart Association. ArteriosclerThromb 14:840–856.

Tatsumi TO, Tanaka Y, Kondoh K, Minohara S, Sawada Y, Tsuchida T, Tajima S, Sasaki S. 1996. Descending branch of lateral femoral circumflex artery as a free graft for myocardial revascularization: a case report. J ThoracCardiovascSurg 112:546–547.

Tubbs RS, Loukas M. 2006. An unusual formation of the deep palmar arch. ClinAnat 19:708–709.

van Son JA, Smedts F, Vincent JG, van Lier HJ, Kubat K. 1990. Comparative anatomic studies of various arterial conduits for myocardial revascularization. J ThoracCardiovascSurg 99:703–707.

Vazquez MT, Murillo J, Maranillo E, Parkin I, Sanudo J. 2007. Patterns of the circumflex femoral arteries revisited. Clin Anat 20:180–185.

Wendler O, Hennen B, Demertzis S, Markwirth T, Tscholl D, Lausberg H, Huang Q, Dübener LF, Langer F, Schäfers HJ. 2000. Complete arterial revascularization in multivessel coronary artery disease with 2 conduits (skeletonized grafts and T grafts). Circulation 102:III79–III83.

Wharton SB, Cary NRB, Gresham GA. 1994. Observations on detailed histology of the internal thoracic artery and their relevance to its comparatively low incidence of atheroma. ClinAnat 7:215–218.

Windecker S, Kolh P, Alfonso F, Collet JP, Cremer J, Falk V, Filippatos G, Hamm C, Head SJ, Jüni P, Kappetein AP, Kastrati A, Knuuti J, Landmesser U, Laufer G, Neumann FJ, Richter DJ, Schauerte P, Sousa UM, Stefanini GG, Taggart DP, Torracca L, Valgimigli M, Wijns W, Witkowski A. 2014. ESC/EACTS Guidelines on myocardial revascularization: The Task Force on Myocardial Revascularization of the European Society of Cardiology (ESC) and the European Association for Cardio-Thoracic Surgery (EACTS)Developed with the special contribution of the European Association of Percutaneous Cardiovascular Interventions (EAPCI). Eur Heart J 35:2541–2619.

Wooten C, Hayat M, du Plessis M, Cesmebasi A, Koesterer M, Daly KP, Matusz P, Tubbs RS, Loukas M. 2014. Anatomical significance in aortoiliac occlusive disease. ClinAnat 27:1264–1274.

Yamashita Y, Fukuda S, Kigawa I, Wanibuchi Y. 2005. Preoperative angiographic evaluation of the descending branch of the lateral femoral circumflex artery as a free graft in coronary artery bypass graft. Jpn J ThoracCardiovascSurg 53:477–480.

Původní práce

Studie morfologie r. descendens a. circumflexae femoris lateralis jako možné cévní náhrady pro rekonstrukci koronárního řečiště pomocí angio CT vyšetření

P. Loskot[1,2], J. Baxa[3], T. Hájek[1], J. Valenta[2]

[1]Kardiochirurgické oddělení FN Plzeň, primář: MUDr. T. Hájek
[2]Anatomický ústav LF UK v Plzni, vedoucí: Doc. RNDr. P. Fiala, CSc.
[3]Klinika zobrazovacích metod LF UK a FN v Plzni, přednosta: Prof. MUDr. B. Kreuzberg, CSc.

Souhrn

Úvod: Vzhledem k potřebě alternativních tepenných štěpů vhodných k rekonstrukci koronárního řečiště jsme provedli morfologickou analýzu ramus descendens arteriae *circumflexae femoris lateralis (RDACFL)* pomocí AGCT vyšetření.

Materiál a metodika: Byly sledovány nejen anatomické variace a kvantitativní zastoupení sklerotických změn, ale i přítomnost kolaterálního systému při významném stenotickém postižení pánevního a femorálního tepenného systému.

Výsledky: Výsledkem je příznivý nález ve smyslu délky námi sledované cévy (průměrně 9,3 cm), relativně malá anatomická variabilita a velmi malé procento sledovaných cév podílejících se na kolaterálním oběhu, přestože v 72 % vyšetření bylo zjištěno významné stenotické postižení (stenóza více než 50 %) horního úseku tepen DK.

Závěr: Cév vhodných k odběru dle zadaných kritérií bylo 68 %. Předpokládáme, že u pacientů bez ICHDK nebo jen s nevýznamnou ICHDK by bylo toto číslo mnohem vyšší.

Klíčová slova: ramus descendens arterie circumflexae femoris lateralis – tepenná revaskularizace myokardu – Y-štěp

Summary

Loskot P, Baxa J, Hajek T, Valenta J. A study of the morphology of the descending branch of the lateral circumflex femoral artery (DBLCFA) as a possible vascular graft for the reconstruction of coronary arteries using angio CT

Introduction: Due to the need for alternative arterial grafts suitable for the reconstruction of the coronary bloodstream, we conducted a morphological analysis of the descending branch of the lateral circumflex femoral artery (DBLCFA) using an AGCT scan.

Material and methods: Not only anatomical variations and the quantitative representation of sclerotic changes, but also the presence of a collateral system in the event of significant stenosis of the pelvic and femoral artery system were analysed.

Results: The results revealed favorable findings in the sense of the studied artery's length (9.3 cm on average), a relatively low anatomical variability and a very small percentage of the studied blood vessels participating in collateral blood flow, despite that 72% of tests revealed significant stenotic disease (stenosis of more than 50%) of the upper branch of lower limb arteries.

Conclusion: According to the defined criteria, 68% of vessels were found to be suitable for grafting. We suppose that this number would be considerably higher in patients with only insignificant or no ischemic disease of the lower extremities.

Key words: descending branch of lateral circumflex femoral artery – arterial revascularization of the myocardium – Y-graft

Rozhl Chir 2014;93:307–310

ÚVOD

V poslední době roste zájem o kompletní nebo částečné tepenné revaskularizace myokardu, především u mladších pacientů. To je dané prokazatelně delší průchodností tepenného štěpu ve srovnání se štěpem žilním [1,2].

Dalším důvodem je relativní nedostatek kvalitních štěpů u polymorbidních nemocných. Proto jsme se zaměřili na nový tepenný štěp, který lze u vybraných pacientů použít jako alternativu.

Tato tepna – ramus descendens arterie circumlexae femoris lateralis (RDACFL) – byla poprvé použita již v roce 1996 [11]. Jedná se o svalovou větev, která se nachází v hloubce mezi hlavami m. quadriceps femoris (Obr. 1).

Studie má několik větví. V tomto sdělení se budeme zabývat morfologií cévy popsanou s využitím AGCT vyšetření (Obr. 2).

Cílem studie je popsat anatomické variety RDACFL, zhodnotit makroskopický stupeň postižení sklerotickým procesem [3,5] a zjistit význam cévy pro vytváření kolaterálního oběhu [8,9,10] při stenotickém postižení pánevního a stehenního řečiště.

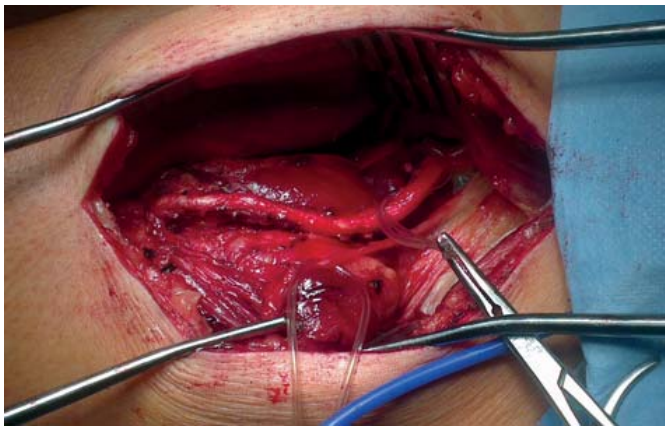

Obr. 1: RDACFL mezi hlavami m. quadriceps fem
Fig. 1: DBLCFA passing between quadriceps muscle heads

Obr. 2: CT zobrazení RDACFL (označena šipkou)
Fig. 2: CT scan of DBLCFA (arrow)

MATERIÁL A METODIKA

Vyšetřili jsme 100 konsekutivních pacientů, 80 mužů (80 %) a 20 žen (20 %), u kterých bylo z nějakých důvodů (nejčastěji ICHDK) indikováno AGCT tepen dolních končetin. Při vyšetření jsme se zaměřili na zobrazení RDACFL. Přednostně (vzhledem k preferovanému chirurgickému přístupu) jsme vybírali LDK (91 %) v 9 případech (9 %) byla zobrazena PDK.

Všechna vyšetření byla provedena v rozsahu břišní aorty, pánevních tepen a dolních končetin na přístroji se dvěma zdroji záření, Somatom Definition Flash (Siemens Healthcare, Erlangen, Německo). Při kolimaci 128x0,6 mm a periodě rotace rentgenky 500 ms byla použita hodnota pitch faktoru 0,9. Expozice byla provedena za použití principu anatomické modulace expozičních parametrů (CarekV a CareDose4D, Siemens Healthcare, Erlangen, Německo) s nastavením referenční hodnoty mAs 120–140. Při vyšetření bylo aplikováno 80 ml jodové kontrastní látky o koncentraci 400 mgI/ml rychlostí 6 ml/s a záplachem 50 ml fyziologického roztoku stejnou rychlostí. Pro hodnocení byla hrubá data rekonstruována do 2 sérií (3 mm a 0,75 mm) s rekonstrukčním filtrem pro zobrazení tepen (B26f).

Hodnocení a měření bylo prováděno na multifunkční stanici Leonardo (Siemens Healthcare, Erlangen, Německo) pomocí softwarové aplikace Syngo Inspace. Nejprve byla provedena segmentace s vytvořením zakřivené multiplanární rekonstrukce v rovině proudnice tepny a následně změření délky RDACFL.

Sledované parametry studie byly následující:

Délka tepny měřená 10 mm od odstupu do terminální bifurkace (event. do průměru 2 mm) a vzdálenost spina iliaca anterior superior k hornímu okraji patelly.

Přítomnost stenózy kmenového řečiště (větší než 50 %) – od oblasti distální břišní aorty (AA) ke společné femorální tepně (AFC) a stenózy povrchové (AFS) a hluboké femorální tepny (AFP).

Sklerotické změny kvantifikované do celkem 5 skupin (0–4), kdy 0 znamená bez sklerotických změn, 1 pouze jemné změny, 2 nevýznamné kalcifikace, 3 sklerotické změny se stenózami na hranici významnosti (minimálně v jednom úseku) a 4 významné sklerotické postižení s významnou stenózou (minimálně v jednom úseku).

Anomální odstup cévy, vysoké větvení, jiná cévní variabilita.

Přítomnost kolaterálního systému, respektive kdy RDACFL tvoří významnou kolaterálu pro tepenné zásobení DK.

VÝSLEDKY

Ze studie vyplývá, že průměrná délka RDACFL dle CTAG kritérií (céva s nativním průtokem bez dilatace) je 9,3. Tato délka je dostatečná při použití štěpu v kardiovaskulární chirurgii. Především v kombinaci s LIMA (left internal mammary artery) je použitelná jako Ygraft [2,3,11] pro revaskularizaci koronárních cév v oblasti přední a boční stěny myokardu.

Nepotvrdil se náš předpoklad, že s délkou stehna (tělesnou výškou) bude růst i délka štěpu. Je zde zřejmá nezávislost (Tab. 1, Graf 1).

Přestože většina vyšetřovaných pacientů měla nějaký stupeň ICHDK [7,8,10], byl pouze v šesti případech vytvořen kolaterální oběh přes RDACFL. V celkem devíti případech se jednalo o hypoplastickou nebo gracilní cévu. Ostatní zjištěné anatomické variety, jako je anomální odstup nebo vysoké větvení, popř. silné svalové větve, neomezují chirurgickou dostupnost štěpu.

Ze 100 vyšetřovaných pacientů mělo 72 (72 %) významně skleroticky postižené pánevní nebo stehenní řečiště (stenóza větší než 50 %, Tab. 3). V 15 případech by nebylo možné tepnu odebrat (6krát byla RDACFL významnou kolaterálou a 9krát se jednalo o gracilní cévu, Tab. 2). V 19 případech měla céva významné aterosklerotické postižení (stupeň 3 a 4). Z toho jedenkrát se zároveň jednalo o výrazně gracilní cévu a v jednom případě tvořila kolate-

Tab. 1: Měření délky RDACFL a délky stehna
Tab. 1: Measuring Length of DBLCFA and Thigh

Celkem	Mužů	Žen	SIAS horní okraj pately	Délka štěpu Od bifurkace do průměru 2mm
100	80 (80 %)	20 (20 %)	Hodnoty od 38,6 do 54,5 cm	Hodnoty od 2,1 do do 17,4 cm
Průměrný věk	69	66	Průměrně 46,16 cm	**Průměrně 9,30 cm**
Průměrná výška (cm)	171,8 (150–197).			
Průměrný BMI	BMI 28,1 (19,1–27,2)			

Tab. 2: Anatomická variabilita cévy – výsledky
Tab. 2: Anatomical variability of vessel – results

Hypoplastická céva	Gracilní pod 2mm při odstupu	Odstup z AFS	Odstup z AFP	Vysoká bifurkace nebo několik silných svalových větví	Kolaterální oběh přes RDACFL
8x	1x	4x	2x	2x	6x (1x při uzávěru AFS)

Tab. 3: Stenotické postižení cév – výsledky
Tab. 3: Stenotic disability of vessel – results

Stenóza AFP více než 50 %	Stenóza AFS více než 50 %	Stenóza mezi aortou a AFC více než 50 %	Významná stenóza na pánevním nebo stehenním řečišti celkem	Významné sklerotické změny RDACFL (st. 3 a 4)
2x	50x	50x	72x	19x

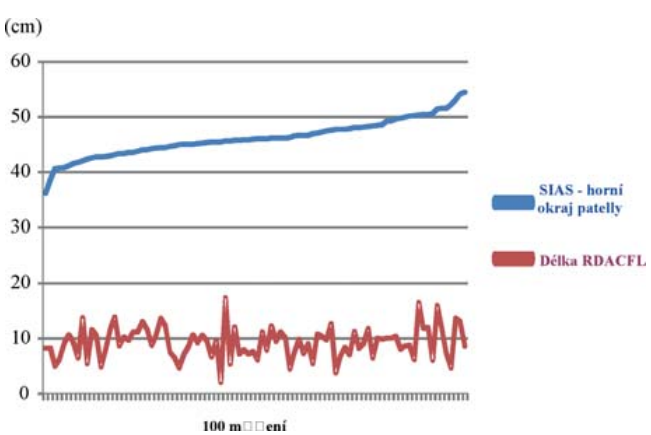

Graf 1: Nezávislost mezi délkou DK a délkou RDACFL
Graph 1: Independence between lower limb length and DBLCFA length

rálu. Celkově lze tedy říci, že ze sledovaného souboru by tepna nebyla vhodná k odběru v 32 případech. Tento výsledek, vzhledem k významnému aterosklerotickému postižení tepen DK, považujeme za velice slibný.

DISKUZE

V současné době jsou klasickými štěpy pro revaskularizaci koronárního řečiště povrchní žíly dolní i horní končetiny a a. mammaria (thoracica) interna. Tepenné náhrady mají dlouhodobě lepší výsledky, a proto se hledají i alternativní tepenné štěpy (a. radialis aj.). Málo používaným alternativním štěpem je sestupná větev a. circumflexa femoris lateralis vzhledem k tomu, že je poměrně hluboko uložena a její kvalitu lze před odběrem obtížně odhadovat. Proto jsme se zaměřili na podrobnější hodnocení této větve z hlediska využitelnosti pro založení aortokoronárního bypassu. V této práci jsme hodnotili anatomicko- morfologické vlastnosti štěpu. V současné době se zaměřujeme na sledování histologických vlastností cévy u vzorků nejen nativních (při koronární revaskularizaci), ale i ze sekčního materiálu. V neposlední řadě sledujeme krátkodobou průchodnost štěpu pomocí AGCT. Celkem byl tento štěp odebrán a použit v 15 případech v průběhu posledních 15 měsíců. Z tohoto počtu jsme štěp nepoužili v jednom případě (příliš gracilní céva) a v jednom případě jsme museli reoperovat pro časný uzávěr štěpu. Dle AGCT koronárních bypassů s odstupem cca 2 měsíců od výkonu se zatím potvrdil v jednom případě uzávěr RDACFL. Někteří autoři [4] uvádějí použitelnost RDACFL u klinicky manifestované ICHDK pouze 10 %. V naší studii je céva vhodná k odběru u 68 pacientů (68 %). Z výše uvedených dat je zřejmé, že použití tohoto štěpu je vhodné u pacientů bez ICHDK. Odběr jsme provedli pouze u pacientů, kteří neměli žádné klinické projevy ICHDK

a měli kvalitní pulzace v tříslech a na periferních tepnách DK. V případě známého ICHDK a především u již vyjádřených klinických obtíží je vhodné v případě uvažování o odběru tohoto štěpu doplnit angiografické vyšetření tepen dolních končetin [3,6].

ZÁVĚR

Z uvedených dat vyplývá, že po morfologické stránce je sledovaná tepna, sestupná větev a. circumflexa femoris lateralis, vhodná k odběru jako tepenný štěp pro konstrukci koronárního bypassu. Rovněž z chirurgického hlediska je její odběr poměrně jednoduchý. Z hlediska kvalitativního hodnocení aterosklerotického procesu RDACFL v porovnání se sklerózou velkých tepen pánevního a stehenního řečiště je tato větev jednoznačně výrazně méně tímto procesem zasažena [6,7,8,9]. Nicméně se domníváme, že odběr není vhodný u pacientů s ICHDK především u jejích těžších forem, z důvodu možného sklerotického postižení nebo možného přerušení kolaterálního oběhu při uzávěru nebo významných stenózách především v povodí AFS.

Náš původní předpoklad, že délka tepny bude přímo úměrná délce stehna (tělesné výšce), se nepotvrdil, je tedy možno uskutečnit odběr prakticky u všech pacientů bez ICHDK. Námi prokázaná průměrná použitelná délka štěpu se pohybuje okolo 9,3 cm. Někteří autoři [3,11] uvádějí délku štěpu až 16 cm, což se ukazuje spíše výjimkou.

LITERATURA

1. Lisboa LAF, Dallan LAO, Puig LB, Filho CA, Leca RC, et al. Midterm follow-up with exclusive use of arterial grafts in complete myocardial revascularization of patients with triple vessel coronary artery disease. Rev Bras Cir Cardiovasc 2004,19. Dostupný z www: http://www.scielo.br/scielo.php?script=sci_arttext&pid=S0102-76382004000100004&lng=en&nrm=iso&tlng=en.
2. Tector AJ, Kress DC, Schmahl TM, et al. T-graft: a new method of coronary arterial revascularization. Cardiovasc Surg (Torino) The Journal of Cardiovascular Surgery 1994; 35(6 Suppl 1):19–23.
3. Fabbrocini M, Fattouch K, Camporini G, DeMicheli G, Bertucci C, et al. The descending branch of lateral femoral circumflex artery in arterial CABG: early and midterm results. The Annals of Thoracic Surgery 2003;75:1836–41.
4. Sakakibara Y, Abe M, Hiramatsu Y, Shigeta O, Ishikawa S, el al. The descending branch of the lateral femoral circumflex artery for coronary artery bypass grafting. The Journal of Thoracic and Cardiovascular Surgery 1999;118:753–754.
5. Lee DH, Lee W, Kim KB, Cho KR, Park EA, et al. Availability of the right gastroepiploic artery for coronary artery bypass grafting: preoperative multidetector CT evaluation. Int J Cardiovasc Imaging 2010;26(Suppl 2):303–10.
6. Met R, Bipat S, Legemate DA, Reekers JA, Koelemay MJ. Diagnostic performance of computed tomography angiography in peripheral arterial disease: a systematic review and meta-analysis. JAMA 2009;301:415–24.
7. Kim JS, Lee HS, Jang PY, Choi TH, Lee KS, et al. Use of the descending branch of lateral circumflex femoral artery as a recipient pedicle for coverage of a knee defect with free flap: anatomical and clinical study. Microsurgery 2010;30:32–6.
8. Sabalbal M. Descending branch of the lateral circumflex femoral artery – arterial genicular anastomoses 2010. Dostupný na www: http://works.bepress.com/sabalbal/2.
9. EG, Taylor HOB, Orgill DP. Patency of the descending branch of the lateral circumflex femoral artery in patients with vascular disease. Plastic and reconstructive surgery 2008;121121–9.
10. Taha HM, Umraz Khan U. The descending branch of the lateral circumflex femoral artery: a reliable and robust alternative blood supply in the free fibular transfer for avascular necrosis of hip. European Journal of Plastic Surgery 2012;35:731–734.
11. Yamashita Y, Fukuda S, Kigawa I, et al. Preoperative angiographic evaluation of the descending branch of the lateral femoral circumflex artery as a free graft in coronary artery bypass graft. Jpn J Thorac Cardiovasc Surg 2005;53:477–80.

MUDr. Petr Loskot
FN Plzeň
alej Svobody 80
304 60 Plzeň
e-mail: loskotp@fnplzen.cz

Alternativní autologní tepenný štěp v kardiovaskulární chirurgii

Loskot P., Široký J., Hájek T., Valenta J.*

Kardiochirurgické oddělení FN Plzeň, primář MUDr. T. Hájek
*Anatomický ústav LF UK Plzeň, vedoucí doc. RNDr. P. Fiala, CSc.

Souhrn

Loskot P., Široký J., Hájek T., Valenta J.: Alternativní autologní tepenný štěp v kardiovaskulární chirurgii

Tepenná revaskularizace myokardu je preferovaná metoda při chirurgické léčbě ischemické choroby srdeční. Jeden z možných alternativních autologních tepenných štěpů je ramus descendens arteriae circumflexae femoris lateralis (RDACFL). Na našem pracovišti (od roku 2003) jsme zatím odebrali a použili 12 těchto štěpů. Všechny štěpy byly použity jako Y-štěp do *arteria mammaria sinistra* k revaskularizaci cílových tepen na boční a spodní stěně srdeční. Průchodnost štěpu byla kontrolována po 3 měsících pomocí angio-CT. Při kontrole byl 1 štěp uzavřen, což znamená více než 91% průchodnost po 3 měsících. Dále nebyly zaznamenány jiné komplikace (problematické hojení rány, parestezie končetiny, krvácení, spazmus štěpu, infekce atd.) v souvislosti s odběrem štěpu. RDACFL je kvalitní alternativní štěp využitelný k tepenné revaskularizaci myokardu.

Klíčová slova: revaskularizace myokardu – tepenné štěpy – Y-štěp

Summary

Loskot P., Široký J., Hájek T., Valenta J.: Alternative Autologous Arterial Graft in Cardiovascular Surgery

Arterial revascularization of myocardium is a method of choice for surgical treatment of ischemic heart disease. The descending branch of lateral femoral circumflex artery (DBLFCA) is one of possible alternative autologous arterial grafts. Up to now, since2003, 12 of these grafts have been harvested and used for revascularization of myocardium at our department. All grafts have been used as a Y-graft to the left internal mammary artery for revascularization of target vessels on lateral and inferior heart wall. Graft patency was controlled by the angio-CT procedure after three months. One of the grafts was occluded at the control. It means patency rate after three months was more than 91%. No other complications (such as problematic wound healing, paraesthaesia of lower leg, bleeding, spasm of the graft, infection etc.) were observed with graft harvesting. DBLCFA is a high-quality and safe alternative arterial graft, available for arterial revascularization of myocardium.

Key words: revascularization of myocardium –arterial grafts – Y-graft

Rozhl. Chir., 2010, roč. 89, č. 8, s. 501–503.

ÚVOD

V poslední době je v kardiochirurgii stále větším trendem preferovat tepenné revaskularizace kompletní i inkompletní, vzhledem k přesvědčivému benefitu pro pacienta [1, 2]. To sebou samozřejmě přináší i problematiku nalezení dostatečného množství kvalitních autologních tepenných štěpů. Kromě již tradičně používaných štěpů jako jsou *a. thoracica interna* (LIMA, RIMA) a *a. radialis* (RA), se dnes používají i štěpy méně obvyklé – *a. gastroepiploica dx.* (rGEA) nebo vzácně *a. epigastrica inf.* (EA) a dnes již nepoužívané *a. subclavia* a *a. lienalis*.

Kompletní tepenná revaskularizace myokardu [1, 3, 4] je časově náročnější, pracnější a technicky obtížnější ve srovnání s tradiční revaskularizací, tedy kombinací tepenných a žilních štěpů. Hledání alternativních tepenných autologních štěpů je i v určitém směru zanedbávaným tématem, protože není lukrativním firemním zájmem a s tím souvisí i nižší finanční podpora výzkumu a publikování odborné literatury. Zdá se, že kompletní tepenná revaskularizace přináší benefit „pouze“ pro pacienta. Vzhledem k pracnosti a časově náročnějšímu výkonu byl celkový počet kompletních tepenných revaskularizací v roce 2002 v EU pouze 1,8 % [3], z celkového počtu revaskularizací myokardu.

Otázkou je, zda potřebujeme nový alternativní štěp. Žilní štěpy nelze použít u pokročilých varikózních změn, po operaci varixů, při těžké chronické žilní insuficienci, těžké ICHDK, hluboké žilní trombóze, *ulcus cruris*, při reoperacích atd. Tepenné štěpy jsou nedostupné v případě reoperací (LIMA, RIMA), při oboustranně pozitivním Allenově testu (RA) a po břišních operacích (rGEA). Můžeme tedy konstatovat, že nový tepenný štěp někdy potřebujeme.

MATERIÁL A METODA

Zaměřili jsme se na *ramus descendens a. circumflexae femoris lateralis* (DBLFC) [5, 6, 7, 8], což je relativně nenápadná tepna v oblasti stehna. Je to jedna z hlubokých větví, určená k zásobení především hlubokých částí čtyřhlavého stehenního svalu.

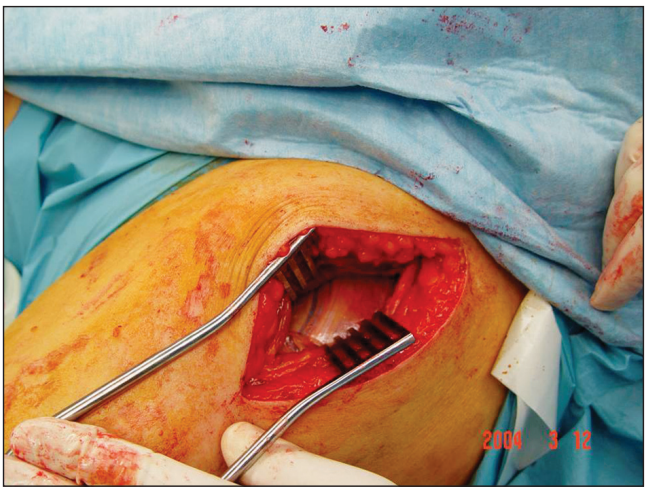

Obr. 1.

Odběr tepny provádíme z anterolaterální svislé incize na stehnu, pod *spina iliaca ant. sup.* o délce asi 15 cm (Obr. 1). Zde pronikneme pod svalovou fascii mezi *m. rectus femoris* a *vastus lateralis*, kde je na *vastus intermedius* uložen nervově cévní svazek. Odebíráme tepnu i s doprovodnými žilami, bez skeletizace (výrazný sklon ke spasmu, Obr. 2) a muskulární nervovou větev pokud možno necháváme *in situ*. Proximálně podvazujeme cévu asi 1–2 cm pod bifurkací z kmene *a. circumlexa fem. lat*. Distální část je ukončena inzercí cév do svalu. Dále se u štěpu označí distální nebo proximální konec a céva se dilatuje – nejlépe papaverinem.

VÝSLEDKY

Všechny námi uskutečněné odběry byly z levého stehna, bez anatomických odchylek. Průměrný čas odběru byl 25 min. (16–41), průměrná délka štěpu 11 cm a distální diametr po dilataci papaverinem průměrně 2,2 mm. Všechny štěpy byly bez aterosklerotických plátů a s pravidelným lumen.

Obr. 2.

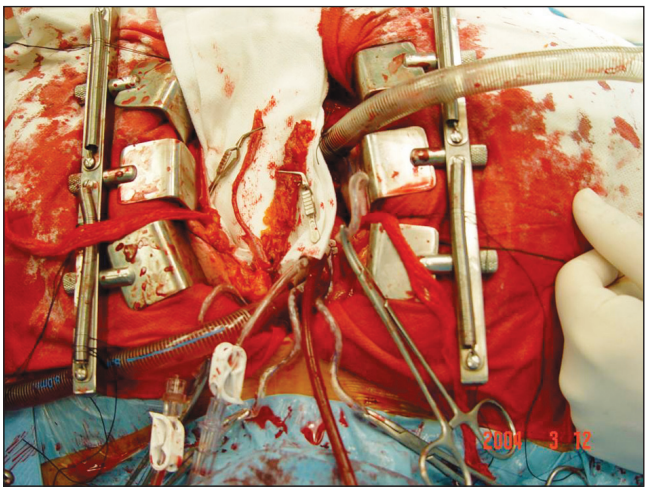

Obr. 3.

Na našem pracovišti jsme zatím odebrali a použili k přemostění koronárních cév 15 těchto štěpů, v rozmezí 10/2003 – 5/2004. Byli to selektivně vybraní pacienti, indikovaní pro ICHS k tepenné (mladší pacienti, nebo nedostatek jiných štěpů) revaskularizaci myokardu. Všechny štěpy byly použity jako Y-graft ad LIMA (Obr. 3) na cílové tepny *ramus diagonalis* (RD, 8x), *r. marginalis sin.* (RMS, 6x) a *r. interventricularis posterior* (RIVP, 1x).

V šestiměsíčním sledování se nevyskytla žádná z těchto komplikací: hojení rány, ischemie kyčle, parestezie DK, krvácení, spazmus štěpu a infekce. V jednom případě jsme provedli evakuaci pozdního hematomu z rány (punkce) a podle AG CT kontroly po 3 měsících, byl jeden štěp uzavřen, to znamená 91,7% průchodných štěpů při krátkodobém sledování.

DISKUSE

Domníváme se, že RDACFL není vhodné odebrat jako tepenný graft u těžkých forem ICHDK a u femoropopliteálních uzávěrů, kde je tato tepna součástí důležitého kolaterálního průtoku. Vhodné je zvážit odběr u pacientů s výškou pod 160 cm (délka štěpu?), u extrémně obézních osob a u pacientů po operacích v lokalitě stehna (TEP, předchozí cévní rekonstrukce atd.). Vhodné je dále zvážit odběr RDACFL při nepoužití prsní tepny nebo při jejím sporném průtoku. Celkové výsledky jsou srovnatelné s pracemi citovaných zahraničních pracovišť.

ZÁVĚR

Ramus descendent a. circumlexae femoris lateralis je kvalitní tepenný štěp, použitelný k revaskularizaci myokardu jako štěp „druhé volby“. Výhodou je snadný odběr, vhodné anatomické uložení a snadná manipulace se štěpem. Štěp vzhledem ke své lokalitě musí být vždy využit jako volný (free graft). Další výhodou je vysoká bez-

pečnost odběru, velmi nízké procento komplikací a krátká doba výuky odběru (learning curve), kdy maximální doba odběru byla 41 minut.

Z našich zkušeností je zatím zřejmé, že štěp má dostatečnou délku i průměr a je tedy vhodný k doplnění chybějících tepenných štěpů. Štěp má velmi dobrou střednědobou průchodnost (více než 91%). Dlouhodobá průchodnost je zatím předmětem dalšího sledování.

LITERATURA

1. **Formica, F., Ferro, O., Greco, P., Martino, A., Gastaldi, D., Paolini, G.** Long-term follow-up of total arterial myocardial revascularization using exclusively pedicle bilateral internal thoracic artery and right gastroepiploic artery. Eur. J. Cardiothorac. Surg., 2004; 26: 1141–1148.
2. **Ferrari, E. R., von Segesser, L. K.** Arterial grafting for myocardial revascularization: how better is it? Current opinion in cardiology. 01/12/2006; 21(6): 584–588.
3. **Oster, H., Schwarz, F., Störger, H., Hofmann, M., Piancatelli, C., Thomas, J., Haase, J.** One-Year Clinical Outcomes After Complete Arterial Coronary Revascularization.. Journal of Interventional Cardiology, Volume 18, Number 6, December 2005, pp. 437–440(4)4.
4. **Baskett, R. J., Cafferty, F. H., Powell, S. J., Nashef, S. A.** Total Arterial Revascularizatio Is Safe: An Analysis Of 71,470 Cases Of Isolated CABG 1992–2001, Cambridge, Massachusetts, USA, Canadian Cardiovascular Congress 2004.
5. **Yuzuru Sakakibara, Masakazu Abe, Yuji Hiramatsu, Osamu Shigeta, Shigemi Ishikawa, Tomoaki Jikuya, Toshio Mitsui, Tsukuba** The Descending Branch Of The Lateral Femoral Circumflex Artery For Coronary Artery Bypass Grafting. J. Thorac. Cardiovasc. Surg., 1999; 118: 753–754.
6. **Fabbrocini, M., Mercogliano, D., Camprini, G., Cioffi, P.** The Descending Branch Of Lateral Femoral Circumflex Artery (DBLFCA) In Arterial Coronary Artery Bypass Grafting. Arterial Conduits For Myocardial Revascularization 19–21 June, 2003 – Rome, Italy.
7. **Toyama Masato, Tamura Yamato, Okiyama Mitsunori, Tsuda Tomohiro** Re-do Coronary Artery Bypass Grafting with the Descending Branch of the Lateral Femoral Circumflex Artery in a Patient with Chronic Hemodialysis Japanese Journal of Thoracic Surgery, vol. 56; No. 12; p. 997–999 (2003).
8. **Široký, J., Hájek, T., Loskot, P., Ferda J.** Descendentní větev arteria circumflexa femoris lateralis – nový štěp pro tepennou revaskularizaci, Sborník abstrakt, I. sjezd České společnosti kardiovaskulární chirurgie Brno, 11. – 12. 11. 2004.

MUDr. Petr Loskot
Sokolovská 88
323 00 Plzeň
e-mail: drlosky@post.cz

Annals of Anatomy 205 (2016) 22–36

Contents lists available at ScienceDirect

Annals of Anatomy

journal homepage: www.elsevier.com/locate/aanat

Research article

Vasa vasorum in the tunica media and tunica adventitia of the porcine aorta

Zbyněk Tonar[a,*], Petr Tomášek[a], Petr Loskot[b], Jiří Janáček[c], Milena Králíčková[a], Kirsti Witter[d]

[a] Department of Histology and Embryology and Biomedical Center, Faculty of Medicine in Pilsen, Charles University in Prague, Karlovarska 48, 301 66 Pilsen, Czech Republic
[b] Department of Anatomy, Faculty of Medicine in Pilsen, Charles University in Prague, Karlovarska 48, 301 66 Pilsen, Czech Republic
[c] Department of Biomathematics, Institute of Physiology Academy of Sciences of the Czech Republic, Videnska 1083, 142 20 Prague, Czech Republic
[d] Institute of Anatomy, Histology and Embryology, Department for Pathobiology, University of Veterinary Medicine Vienna, Veterinärplatz 1, A-1210 Vienna, Austria

ARTICLE INFO

Article history:
Received 1 October 2015
Received in revised form
14 November 2015
Accepted 5 January 2016

Keywords:
Artery
Microvessels
Pig
Stereology
Vascular wall
von Willebrand factor.

ABSTRACT

Vasa vasorum supply both the tunica adventitia and the tunica media of major arteries with nutrients and oxygen. We estimated the density of von Willebrand factor-positive profiles of vasa vasorum visible in transversal histological sections of 123 tissue samples collected from five anatomical positions in the porcine aortae of growing pigs ($n = 25$). The animals ranged in age from 0 to 230 days. The tunica media of the thoracic aorta had a greater vasa vasorum density, with microvessels penetrating deeper towards the lumen than in the abdominal aorta. The density of vasa vasorum gradually decreased with age in both the media and the adventitia. The relative depth into which the vasa vasorum penetrated and where they branched remained constant during the ageing and growth of the media. The ratio of the tunica media and tunica adventitia thicknesses did not change in the single aortic segments during ageing. The media of older animals received fewer but equally distributed vasa vasorum. A greater density of vasa vasorum in the media was correlated with greater media thickness and a greater elastin fraction (data on elastin taken from another study on the same samples). Immunohistochemical quantification revealed deeper penetration of vasa vasorum towards the adluminal layers of the tunica media that were hitherto reported to be avascular. The complete primary morphometric data, in the form of continuous variables, have been made available as a supplement. Mapping of the vasa vasorum profile density and position has promising illustrative potential for studies on atherosclerotic and inflammatory neovascularization, aortic aneurysms, and drug distribution from arterial stents in experimental porcine models.

1. Introduction

Vasa vasorum deliver oxygen and nutrients into and drain metabolites from the wall of larger blood vessels, thus providing essential physiological support for growth, repair, and homeostasis of the vascular wall. Two anatomically distinct distribution patterns of vasa vasorum have been distinguished: (i) the first-order vasa run more or less longitudinally to the host vessel, and (ii) their second-order branches are arranged preferentially spirally or circumferentially (Moreno et al., 2006). Although vasa vasorum occur predominantly in the adventitia, their branches also penetrate into the media of the larger vessels. Conventional studies on aortic vasa vasorum in human and other mammals (Wolinsky and Glagov, 1967, 1969) have shown that in healthy elastic arteries, an inner (adluminal) zone contains no vasa vasorum, as it is supposedly supplied by diffusion from the vascular lumen. This avascular zone has been described to be approximately 0.5-mm thick on average in adults, which corresponds to 29 lamellar units, each of them consisting of vascular smooth muscle cells sandwiched between collagen and elastin fibres and ground substance (thickness of one lamellar unit: approximately 15–16 μm; Shadwick, 1999). These findings have been repeatedly confirmed, thus demonstrating that ontogenesis, the anatomical position of the vessel, local oxygen tension and wall thickness are important determinants of the presence or absence of vasa vasorum (Okuyama et al., 1988). The avascular or less vascularized regions of major arteries, and especially the aorta, have proved to be prone to atherosclerosis (Ritman and Lerman, 2007). In contrast, vasa

* Corresponding author. Tel.: +42 0377593320.
E-mail address: tonar@lfp.cuni.cz (Z. Tonar).

http://dx.doi.org/10.1016/j.aanat.2016.01.008
0940-9602/

vasorum proliferation within the intima and media is a part of the inflammatory response during atherosclerotic plaque development. This arterial neovascularization heavily contributes to leukocyte recruitment, intimal hyperplasia (Newby and Zaltsman, 2000), and the instability of atherosclerotic plaques (Moulton et al., 2003; Moreno et al., 2006; Baikoussis et al., 2011), thus increasing the rupture risk (Fleiner et al., 2004). Moreover, vasa vasorum play a significant role in the pathogenesis of a number of surgical aortic diseases, such as aortic aneurysm (Eberlova et al., 2013), acute or chronic aortic dissection, intramural haematoma, and restenosis after transluminal angioplasty (Baikoussis et al., 2011).

1.1. Visualization of vasa vasorum

In histological sections, larger vasa vasorum are easily identified within the tunica adventitia using overall staining (Okuyama et al., 1988), but for quantitative visualization of all vasa vasorum in the tunica media, staining for specific endothelial markers, such as von Willebrand factor (Witter et al., 2010; Tonar et al., 2012; Houdek et al., 2013; Xu et al., 2015) or CD markers such as CD31 (Eberlova et al., 2013) or CD34, if available for the respective mammalian species (for review, see, e.g., Ordóñez, 2012), is necessary. To overcome the limitations of two-dimensional histological studies, three-dimensional *in vivo* micro-CT imaging (X-ray microtomography) has been used for detailed mapping and spatial reconstruction of the branching pattern of vasa vasorum (Galili et al., 2004; Moreno et al., 2006). These studies have revealed an immense heterogeneity of adventitial vasa vasorum among different vascular beds. Three-dimensional methods also offer a number of quantitative parameters for assessment of the vasa vasorum network, e.g., the volume fraction of vasa vasorum within the wall, the ratio between the second-order and the first-order vasa vasorum, the *in vivo* diameter, or the numerical density of branching points (Galili et al., 2004). Several of these findings were suggested to be helpful for explaining the variable propensity for vascular disease among different vascular beds. An even higher resolution than in *in vivo* can be achieved by micro-CT of microvascular corrosion casts using injections of capillary-passable polymers (Ritman and Lerman, 2007). To assess the vasa vasorum in superficially positioned arteries, contrast-enhanced ultrasound techniques were tested in animal models (Granada and Feinstein, 2008). However, histological studies on vasa vasorum are still valuable because they may be applied to archive material. Additionally, the vasa vasorum can be assessed together with angiogenic or hypoxia markers, and the labelling of vasa vasorum in histological and histopathological sections is very reliable and reproducible and still shows the highest resolution of all available methods.

1.2. Aortic vasa vasorum in experimental porcine models

Due to its size and thickness, anatomical proportions, wall structure, and physiological similarities, the porcine aorta is the most suitable animal model of the human aorta and is currently being used in cardiovascular surgical (Dziodzio et al., 2011; Funder et al., 2012; Saari et al., 2012; Sarda-Mantel et al., 2012; Johnson et al., 2013) and biomechanical (Kim and Baek, 2011; Lillie et al., 2012) studies. Vasa vasorum quantification has been used as a marker of inflammatory neovascularization following reaction of the porcine aortic wall to tissue glues tested for the treatment of aortic dissection (Witter et al., 2010). Similarly, vasa vasorum have been used as a histopathological marker of pharmacologically mitigated progression of experimental aneurysm in the porcine abdominal aorta (Houdek et al., 2013). Nedorost et al. (2013) assessed vasa vasorum not in the aorta, but rather in the pulmonary artery, when examining the histopathological reaction to pulmonary artery banding in a growing porcine model. The porcine aorta was successfully used for testing anti-angiogenic drugs on adventitial neovascularization in experiments regarding early atherosclerotic lesions (Xu et al., 2015). Aguirre-Sanceledonio et al. (2003) investigated vasa vasorum hypertrophy in a porcine model of experimental coarctation of the thoracic aorta, demonstrating anastomoses between vasa vasorum and collateral aorto-aortic anatomical shunts. Angouras et al. (2000) found that after interrupting the vasa vasorum in the thoracic porcine aorta, decreased vasa vasorum blood flow resulted in necrosis, accompanied by elastin and collagen abnormalities in the outer media. The resulting interlaminar shear stresses and increased aortic stiffness were believed to contribute to the development of aortic dissection (Angouras et al., 2000). Mapping of porcine aortic vasa vasorum also has promising potential for explaining the diffusion of macromolecules through the wall of large elastic arteries (Hwang and Edelman, 2002), including the drug distribution from arterial stents with fine control of locally directed drug release (Kusanagi et al., 2007). Moreover, vasa vasorum are important for physiologically relevant porcine aortic models evaluating manufactured endovascular stent-grafts (Desai et al., 2011).

Summarizing the studies cited above, the distribution and quantity of porcine aortic vasa vasorum rely on a number of factors that affect the microenvironment of the media and adventitia. A number of microscopic differences must therefore be assumed to exist along the whole aorta (cf. Sokolis, 2007; Sokolis et al., 2008). However, a detailed study comparing any potential regional and age-related differences in vasa vasorum of the porcine aorta is still missing. None of the studies cited above provided quantitative information on vasa vasorum in the media and adventitia of various aortic segments at the same time. The first rationale for our study was to quantify the immunohistochemically detectable vasa vasorum in various aortic segments and in different age groups of pigs that are frequently used in experiments using statistically comparable variables. As we recently published a quantitative study on segmental and age differences in the elastin network, collagen, and the smooth muscle phenotype in the tunica media of the porcine aorta (Tonar et al., 2015b), we decided to analyse vasa vasorum in parallel sections of the same tissue blocks. Providing quantitative information on vasa vasorum within the context of the aortic wall composition became the second rationale for the present study.

1.3. Study aims

The aim of our study has been to assess the density and distribution of vasa vasorum by immunohistochemical detection in transversal histological sections of the porcine aorta and to compare the data between single aortic segments and between age groups. Moreover, possible correlations between vasa vasorum morphometry and the histological composition of the same aortic samples as published in a previous study (Tonar et al., 2015b) were tested. The following null hypotheses were formulated and tested:

H_0(A): The two-dimensional density of vasa vasorum profiles per section area unit is the same in all proximodistal aortic segments of the same individual when comparing the aortae of growing domestic pigs (age 0–230 days). This was tested separately for the media, adventitia, and whole wall. Due to considerable variations in the thickness of the tunica media observed in our unpublished preliminary studies, the density of vasa vasorum in the media was studied in five artificially defined virtual sublayers in particular, with each of these sublayers comprising one-fifth of the media thickness.

H_0(B): The mean relative position of vasa vasorum profiles within the media and adventitia is the same for suckling piglets, weaners,

and fattening pigs when comparing corresponding aortic segments. This was tested separately for the media and adventitia.
H_0(C): The two-dimensional density of vasa vasorum profiles per section area unit is the same in the adventitia as in all virtual sublayers of the media. This was tested separately for all three age groups and all five aortic segments under study.
H_0(D): The density and the distribution of the vasa vasorum do not correlate with the thickness of the aortic layers or with the histological composition of the porcine aorta, as published previously (Tonar et al., 2015b).

2. Materials and methods

2.1. Animals, specimen preparation, aortic segments, and age groups

We used the aortic samples previously collected for studies on vascular smooth muscle orientation (Tonar et al., 2015a) and the histological composition of the aorta (Tonar et al., 2015b). Whole aortae of domestic pigs were collected. The animals (commercial fattening hybrids, $n = 25$; 12 males, 11 females, 1 castrated male, 1 without documented sex; age 0–230 days; weight 0.7–95 kg) were euthanized at the end of other experiments related to immunology and parasitology (Worliczek et al., 2010; Gabner et al., 2012; Ondrovics et al., 2013). All of the animals were raised conventionally and treated in compliance with the European Convention on Animal Care.

The aortae were without any macroscopic signs of pathological changes. After routine fixation using buffered formalin according to Lillie (Romeis, 1989), the aortae were divided into five aortic segments, each of them representing one of the following regions: the ascending aorta (*aorta ascendens*), aortic arch (*arcus aortae*), thoracic descending aorta (*aorta thoracica*), suprarenal abdominal aorta (*aorta abdominalis*, *pars suprarenalis*), and infrarenal abdominal aorta (*aorta abdominalis, pars infrarenalis*; Fig. 1A). After fixation, the samples were rinsed in 70% ethanol. From each aortic segment, one tissue block was embedded in paraffin for transversal sectioning. To compare the aortic samples according to age, the animals were divided into the following three groups: suckling piglets (age 0–28 days, $n = 64$ vascular segments collected from 13 animals), weaners (age 29–75 days, $n = 35$ vascular segments collected from 7 animals), and fattening pigs (age 180–230 days, $n = 24$ vascular segments from 5 animals). In total, 123 tissue samples were collected (two infrarenal segments were missing because they were damaged during dissection).

2.2. Preparation of histological sections

Two histological sections per sample (section thickness 4 μm) were cut perpendicularly to the longitudinal axis of the vessel. The sections were deparaffinized and rehydrated. In one section, the layers of the aortic wall were identified using a combination of Verhoeff's haematoxylin and green trichrome staining according to Kocova (1970). In the other section, vasa vasorum were detected immunohistochemically using an anti-von Willebrand factor antibody. After blocking the endogenous peroxidase activity in the rehydrated sections with 0.6% H_2O_2 in methanol and following antigen retrieval by protease digestion (1 mg protease from *Streptomyces griseus* (Sigma-Aldrich, Vienna, Austria)/1-ml phosphate-buffered saline (PBS; pH 7.4)) for 20 min at room temperature, unspecific binding activity was blocked with 1.5% normal goat serum (DakoCytomation, Glostrup, Denmark) in PBS for 30 min. Afterwards, the sections were incubated overnight at 4 °C with primary polyclonal rabbit anti-human von Willebrand factor antibody (DakoCytomation). The immunoreaction was detected using the BrightVision Poly-HRP-Anti-rabbit kit (ImmunoLogic, Duiven, The Netherlands) according to the manufacturer's instructions. The reaction was visualized with diaminobenzidine (Sigma-Aldrich, Vienna, Austria) in 0.03% H_2O_2 in PBS. After immunohistochemistry, the sections were counterstained with Mayer's haematoxylin, dehydrated and mounted with a medium soluble in xylene.

2.3. Micrographs

For each section with immunohistochemically visualized vasa vasorum, two micrographs were taken from the opposite sides of the aortic ring using a 4× objective mounted on an Olympus BX51 microscope (Olympus, Tokyo, Japan). The magnification was low enough to capture the whole thickness of the aortic wall, but, at the same time, the micrographs provided a resolution of 1 pixel = 2.2 μm, guaranteeing reliable identification of all immunopositive vasa vasorum. With a total sampled area of 19 mm^2 per section, the whole or a significant part of the aortic section profile was captured by the two micrographs, depending on the anatomical size and wall thickness. The sampling micrographs were randomly positioned on the section, without preferential sampling of the dorsal, ventral, or lateral sides, as the information on anatomical directions was not labelled on the slides. In total, 246 micrographs were captured and analysed from the 123 tissue samples. The sampling of the micrographs from the sections is explained in Fig. 1B.

2.4. Morphometry of vascular layers and of vasa vasorum within the tunica media and adventitia

In each micrograph, three morphologically clearly visible linear border profiles were highlighted (Fig. 1C) using the Multiline tool of Ellipse software (ViDiTo, Košice, Slovak Republic): (i) the section profile of the adluminal surface of the intima (labelled as line 1), (ii) the section profile of the border between the media and the adventitia (labelled as line 2), and (iii) the section profile of the outer (abluminal) border between the adventitia and the periaortic loose connective tissue (labelled as line 3). The media-adventitia border was defined as the most abluminal regularly repeating lamellar unit of the tunica media. The outer adventitial border was defined as the transition between the adventitial dense collagenous connective tissue (counted as the adventitia) and the highly variable surrounding loose periaortic connective tissue (not included in the adventitia). These morphological borders were clearly visible, even in immunohistochemically stained sections. If necessary, the adjacent sections stained with elastic and trichrome stain were consulted to identify the borderlines (not shown). Examples of microvessel identification in the tunica media and tunica adventitia are shown in Fig. 1D and E, respectively.

The thickness of the vascular layers was estimated using the LocalizeInWall2 module of the Ellipse software, as follows: the intima + media thickness was defined as the mean distance between line 1 and line 2 in both sections. This was performed by averaging the shortest connections between the points of both lines. As the intima was very thin and practically indistinguishable from the media, they were counted as part of the same reference area. The adventitial thickness was the mean distance between line 2 and line 3 in both sections. The measurement of wall thickness used in the present study differed from the technique applied in the adjacent sections in the previous study (Tonar et al., 2015a,b). The present technique relied on a much larger sampling area and was immediately linked to the assessment of the vasa vasorum density and distribution in all sections (see below). The profile areas of all of the layers (A(layer)) were calculated.

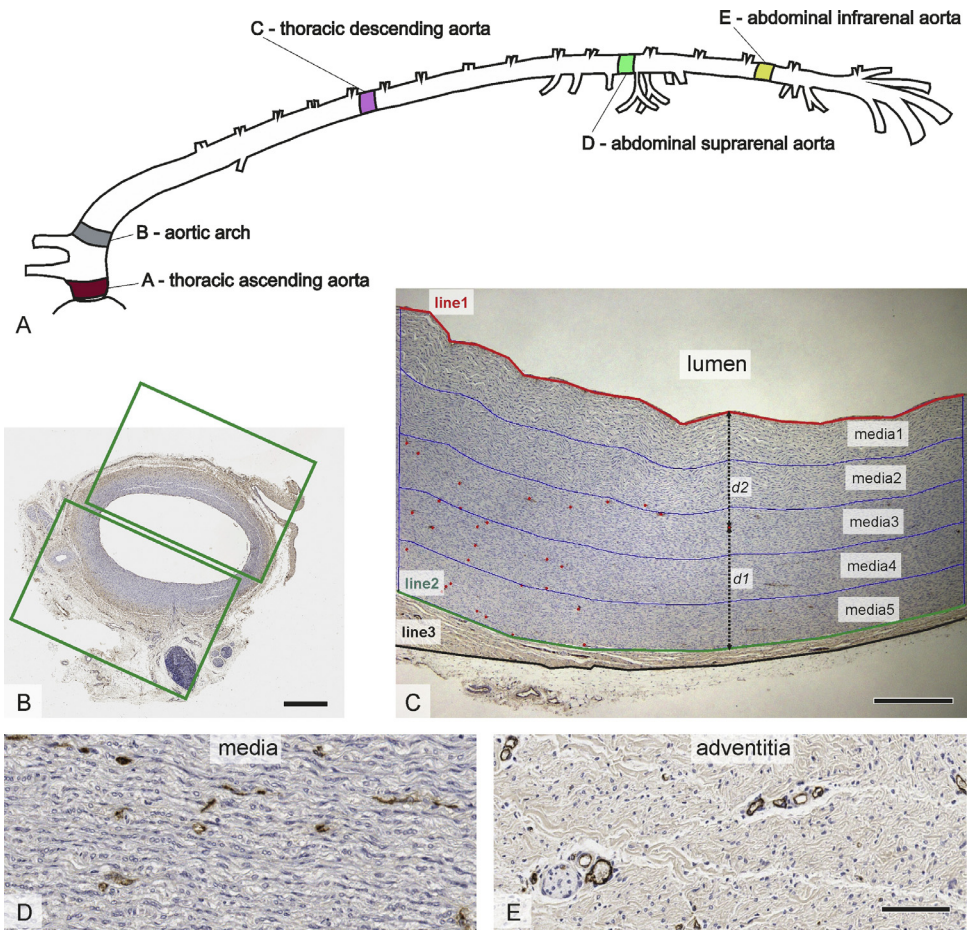

Fig. 1. Position and sampling of the porcine aortic wall and quantitative assessment of the vasa vasorum. (A) Anatomical position of the aortic segments (A–E) collected in the present study. The positions were redrawn according to the anatomical dissection of the porcine aortae (KW) and according to Nickel et al. (1996). Reproduced from Tonar et al. (2015b) with the permission of Elsevier. (B) Two micrographs (demonstrated with proportionally sized rectangles) were taken from the opposite sides of the aorta, recording all of the aortic layers. The pair of the micrographs had no preferential position in relation to the original anatomical directions. (C) The outlines of the aortic wall layers were drawn manually onto the micrographs, with line 1 (red) marking the adluminal surface of the intima, line 2 (green) marking the border between the media and the adventitia, and line 3 (black) outlining the border between the adventitia and the periaortic loose connective tissue. The intima + media thickness was measured as the mean distance between line 1 and line 2. Five virtual sublayers of media (media1 to media5, each comprising 20% of the local thickness) were projected onto the micrograph. The adventitia thickness was the mean distance between line 2 and line 3. The number and position of the vasa vasorum profiles were recorded (marked with red points in the left part of the image, otherwise stained dark brown). The relative position of the profiles within the media was expressed as the ratio between the $d1$ and the $d1 + d2$ distances (see the Section 2 for further details and an assessment of the vessel position in the adventitia). (D) Examples of vasa vasorum in the media. (E) Examples of vasa vasorum in the adventitia. Immunohistochemical detection of the endothelial von Willebrand factor, visualization with horseradish peroxidase/diaminobenzidine (brown), and counterstaining with haematoxylin. Scale bars: 1 mm (B), 500 μm (C) and 100 μm (D,E) (B–E taken from animals of various ages to illustrate the size differences) (For interpretation of the references to color in this figure legend, the reader is referred to the web version of this article).

The position and number of all vasa vasorum profiles within the defined layers were marked and counted using the Point tool of the Ellipse software. Using the LocalizeInWall2 module of the same software, the quantity of vasa vasorum was assessed as the *number of von Willebrand factor-positive microvessel profiles per section area* Q_A of the vascular wall (Witter et al., 2010; Tonar et al., 2012; Eberlova et al., 2013; Houdek et al., 2013):

$$Q_A(\text{microvessels,layer}) = Q/A(\text{layer})\ (\text{mm}^{-2}),$$

where, Q was the number of microvessel profiles counted and A(layer) was the estimated reference area of the section through the aortic wall layers. This was performed separately (i) for the tunica media and intima reference areas and (ii) for the tunica adventitia reference area. Afterwards, the number of microvessel profiles per area unit of the individual layers was summed and related to the total cross-sectional area of the whole aortic section to calculate the mean vasa vasorum density of the whole sample. To assess the depth of vasa vasorum penetration into the media in more detail, five virtual sublayers were arbitrarily defined within the intima + media. Each of these sublayers had an equal thickness comprising exactly 20% of the local intima + media thickness. As the intima contained no microvessels at all, these sublayers of media were numbered media1 to media5, starting from the innermost adluminal sublayer (Fig. 1C).

The relative position of the vasa vasorum profiles within their relevant layers (i.e., their penetration depth) was assessed using an arbitrarily defined function f describing the relative distance of the profiles in the radial direction across the wall: $f = d1/(d1 + d2)$, where, $d1$ was the distance of the vessel profile from the abluminal border of each layer and $d2$ was the distance of the vessel profile from the more adluminal border of the same layer. The value of f equalled 0 at the abluminal border and equalled 1 at the adluminal border of each layer (Fig. 1C).

All quantitative parameters assessed in this study are defined and explained in Table 1. To eliminate the possible edge effect (Gundersen, 1977) and repeated counting of the same vessel profiles crossing the borders between media/adventitia and adventitia/periaortic loose connective tissue, the left adluminal part of the vessel profile was arbitrarily determined to include or exclude

Table 1
Quantitative parameters used in this study for morphometry of vasa vasorum within the porcine aortic wall.

Quantitative parameter abbreviation	Definition, reference area, interpretation and units
Q_A(media)	Number (or two-dimensional density) of vasa vasorum profiles found within the intima and media per area unit of the intima and media in a transverse section of the aorta (mm^{-2}).
f(media)	Mean relative distance of vasa vasorum profiles found within the intima and media from the border between the media and the adventitia. A dimensionless parameter ranging between 0 and 1, where 0 refers to vasa vasorum directly at the media-adventitia border and 1 refers to vasa vasorum on the intraluminal border of the intima (−).
Int + media thickness (IMT)	The combined thickness of the intima and media, measured as the mean distance between the intimal surface profile (Fig. 1C, line 1) and the media-adventitia border profile (Fig. 1C, line 2) (μm).
Q_A(adventitia)	Density of vasa vasorum profiles within the adventitia (mm^{-2}).
f(adv)	Mean relative distance of vasa vasorum profiles in the tunica adventitia from the outer adventitial border (−).
Adventitia thickness (AT)	Thickness of the adventitia, measured as the mean distance between the media-adventitia border (Fig. 1C, line 2) and the outer adventitial border (Fig. 1C, line 3) (μm).
Q_A(wall)	Density of all vasa vasorum profiles per area unit of the whole section profile of the aortic wall (mm^{-2}).
Wall thickness (WT)	IMT summed with the AT (μm).
A_A (elastin, collagen, actin, desmin, and vimentin)	*The area fractions of the elastin, collagen, actin, desmin, and vimentin within the tunica intima and media reference areas (−).*

See also Section 2 and Fig. 1C for further explanation. *The values of the area fractions of the aortic wall constituents (elastin, collagen, actin, desmin, and vimentin) were taken from previously published results analysing the same tissue samples (Tonar et al., 2015b).*

the microvessel profile from the counting. In case of occasional preparation and sectioning artefacts, such as microcracks and folds, the section under study was replaced by adjacent serial section to prevent any bias to the quantification of density and position of the vasa vasorum profiles. Only technically well-prepared sections were eligible for the quantification. In total, 15,070 vasa vasorum profiles were counted (7799 within the intima + media and 7271 within the adventitia reference area).

2.5. Statistics

Shapiro–Wilk's *W*-test was used for normality testing of the data and demonstrated that the distribution of the values differed from the normal distribution in certain aortic segments. Therefore, nonparametric statistics were applied for further analysis. The Friedman ANOVA test for dependent variables and the Wilcoxon matched-pairs test were used to assess the differences between aortic segments (A–E) from the same animals under study and between the aortic layers of the same individuals. The Kruskal–Wallis ANOVA test and the Mann–Whitney U-test were used to assess the differences between the age groups. The correlation between the density and distribution of vasa vasorum profiles, the thickness of the aortic wall layers, and the composition of the tunica media were evaluated using the Spearman correlation coefficient. These tests were used as available in the Statistica Base 11 package (StatSoft, Inc., Tulsa, OK, USA). Significant results are reported as * ($p < 0.05$), ** ($p < 0.01$), and *** ($p < 0.001$).

3. Results

3.1. Segmental differences in the vasa vasorum density and distribution

In the tunica media, differences in both the vasa vasorum profile density and their distribution were found when comparing the values for all aortic proximodistal segments (i.e., from the heart to the terminal branching of the aorta) of the same animal. The density of the vasa vasorum profiles (Fig. 2A) decreased in the proximodistal direction, and highly significant differences were found between nearly all aortic segments under study, except the suprarenal and infrarenal aortae. The mean relative distance of the vasa vasorum profiles from the media-adventitia border was greater in thoracic aortic segments A–C than in abdominal segments D–E and differed between all segments, except between the aorta ascendens and the arcus aortae and between the aorta ascendens and the thoracic descending aorta (Fig. 2B).

In the tunica adventitia, no significant differences were found in either the density or the distribution of the vasa vasorum profiles (Fig. 2C and D).

When considering the mean density of the vasa vasorum profiles calculated per whole wall, the thoracic aortic segments differed from the abdominal segments (Fig. 2E), with the values being greater in the abdominal segments. The ratio of the intima-media thickness to the wall thickness gradually decreased in the proximodistal direction (Fig. 2F).

As expected, no vasa vasorum were found in the most adluminal fifth of the media (media1). When comparing the five virtual sublayers of the media, the proximal segments of the aorta (segments A–C) had greater densities of vasa vasorum profiles in the media2 to media4 sublayers than the abdominal aortic segments (D–E) did (Fig. 3A).

To summarize the segmental differences, the H_0(A) hypothesis was rejected for the tunica media, for most of the virtual sublayers of the media, and for the whole aortic sectional profile, but it was retained for the tunica adventitia.

3.2. Comparison of the vasa vasorum density and distribution between the age groups

Quantitative differences between the age groups are displayed in Fig. 4. In the media, the density of the vasa vasorum profiles was lower in fattening pigs than in sucklings or weaners (Fig. 4A) but retained the same distribution (Fig. 4B). In the adventitia, the density of the vasa vasorum profiles was lower in fattening pigs than in suckling pigs (Fig. 4C), and the distance of the vasa vasorum profiles from the outer border of the adventitia (the penetration depth) decreased with age (Fig. 4D). When considering the mean density of the vasa vasorum profiles calculated per whole wall, it gradually decreased with age (Fig. 4E). The ratio of the intima-media thickness to the wall thickness remained constant during ageing (Fig. 4F).

When comparing the five virtual sublayers of the media, the density of the vasa vasorum within the outermost media5 sublayer showed a significant decrease with age (Fig. 3B).

To summarize the age differences, the H_0(B) hypothesis was rejected for both the density and the distribution of vasa vasorum in the tunica media, in the most abluminal sublayer of the media (media5), in the adventitia, and also in the whole sectional profile of the wall.

3.3. Comparison of the vasa vasorum density between the vascular layers

In all aortic segments (Fig. 5A–E), the adventitia had the greatest density of vasa vasorum profiles, followed by the most abluminal

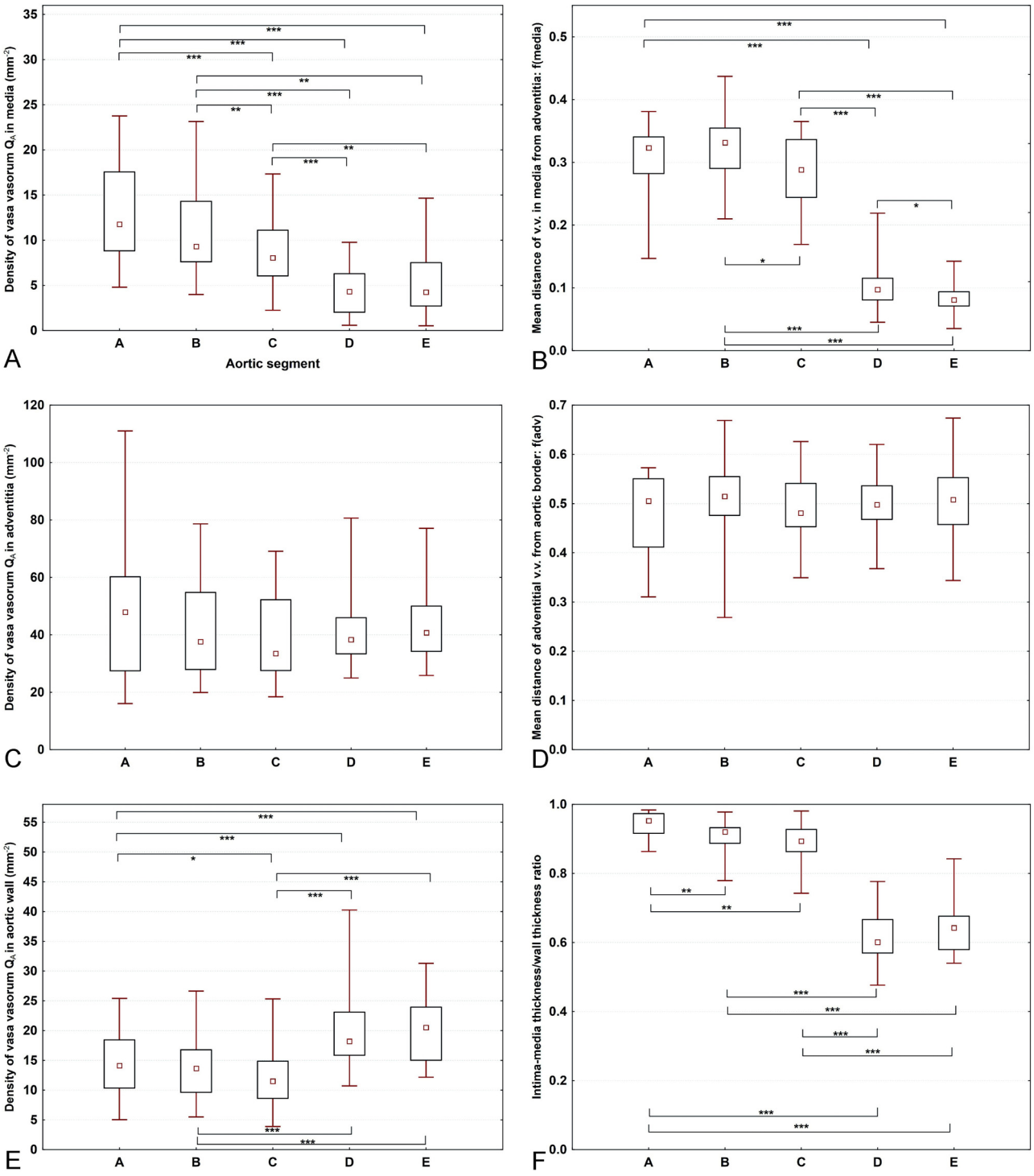

Fig. 2. Density of vasa vasorum (v.v.) profiles (Q_A) in the tunica media (A), the adventitia (C) and the aortic wall (E) of 0–230-day-old pigs, together with the relative position of vasa vasorum profiles within the media (B) and adventitia (D) and the ratio of the intima-media thickness to the whole-wall thickness (F). The relative positions of vasa vasorum profiles were determined as the distance from the outer wall layer divided by the wall layer thickness. Segments A, B, C, D, and E on the *x*-axis denote the aorta ascendens, arcus aortae, thoracic descending aorta, suprarenal abdominal aorta, and infrarenal abdominal aorta, respectively. The age groups were pooled for this comparison. Only the corresponding paired values from the same individuals were tested. The differences between the segments were first tested using the Friedman ANOVA test, which showed significant differences ($p < 0.001$) in the parameters shown under A, B, E, and F. For the parameters shown in A, B, E, and F, the Wilcoxon matched-pairs test was performed to compare the aortic segments (significant *p*-values are presented within the diagrams: * $p < 0.05$, ** $p < 0.01$, *** $p < 0.001$). The data are displayed as the median values, with boxes spanning the upper limits of the first and third quartiles and with whiskers spanning the minimum and maximum values for each group.

sublayer of the media (media5). The density of vasa vasorum gradually decreased towards the adluminal sublayers of the media until it reached zero in the innermost layer (media1). In contrast, the thoracic aorta (Fig. 5A–C) contained vasa vasorum profiles even within the middle sublayers of the media (media3, i.e., 40–60% of the media thickness measured from the intima), and these layers were avascular in the abdominal aortic segments (Fig. 5D–E).

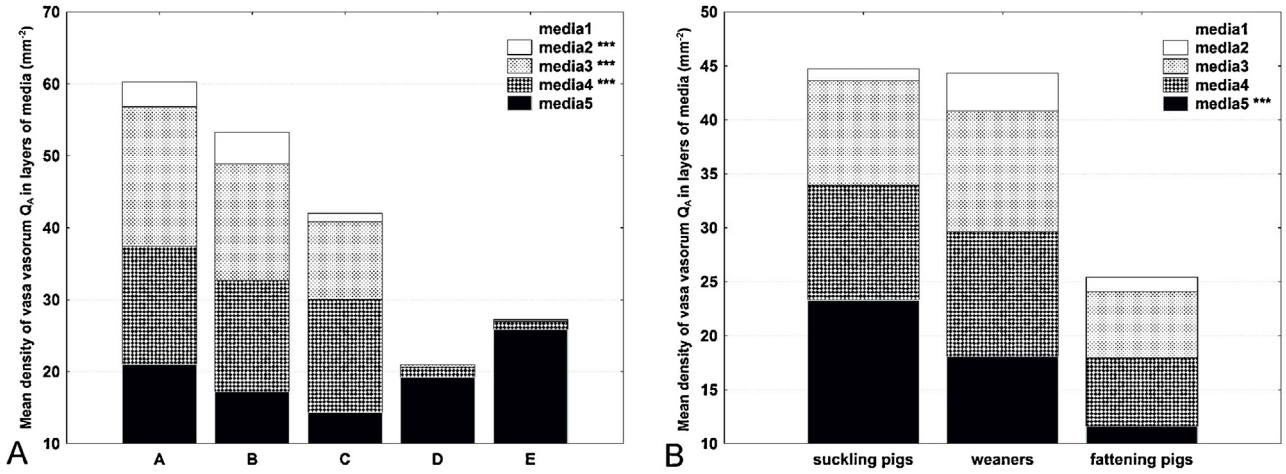

Fig. 3. Mean densities of vasa vasorum profiles within five arbitrary layers of the tunica media and comparison between the porcine aortic segments (A) and between the age groups (B). Segments A, B, C, D, and E on the *x*-axis in (A) denote the aorta ascendens, arcus aortae, thoracic descending aorta, suprarenal abdominal aorta, and infrarenal abdominal aorta, respectively. The data are presented as stacked plots demonstrating the proportions among the individual layers. Each of the media sublayers represented one-fifth of the media thickness. The sublayers were labelled starting from the intimal surface, with media1 and media5 representing the innermost and outermost media layers, respectively. Sublayer media1 did not contain vasa vasorum. (A) The proximal aortic segments (segments A–C) had greater densities of vasa vasorum profiles in the media2 to media4 sublayers than the abdominal aortic segments did (D–E) (*** denotes highly significant differences at $p < 0.001$ in the Friedman ANOVA test). (B) When comparing the age groups, the densities within the outermost media5 sublayer showed a significant decrease in the vasa vasorum density with age (*** denotes $p < 0.001$ in the Kruskal–Wallis ANOVA test).

In all age groups (Fig. 6A–C), the adventitia had the greatest density of vasa vasorum profiles, followed by the most abluminal sublayer of the media (media5). The density of vasa vasorum gradually decreased towards the adluminal sublayers of the media until it reached zero in the innermost layer (media1) in all age groups. No differences were found between the media3 and the media4 sublayers in all groups; i.e., the density of profiles was the same within the middle region of the media (40–80% of the media thickness measured from the intima), independent of age.

To summarize the differences between the layers, the H_0(C) hypothesis was rejected.

3.4. Correlation of the vasa vasorum density and distribution with the thickness of the aortic wall and with the tunica media histological composition

The Spearman rank-order correlations between quantitative parameters that were found to be significant ($p < 0.05$) are listed in Table 2. H_0(D) was rejected, as both the density and the distribution of vasa vasorum in both the media and the adventitia correlated with the thickness of the aortic wall layers as well as with the aortic wall composition.

3.5. Complementary qualitative morphological findings

No direct communication of vasa vasorum with the aortic lumen (vasa vasorum interna) was observed. Examples of segmental and age-related differences in the vasa vasorum profile density and distribution are shown in Fig. 5. Differences in the relative thicknesses of the media and adventitia between the proximodistal aortic segments were clearly visible, even without quantification, but the density estimates were reliably detectable only by quantitative assessment and statistics. However, the deeper penetration of the vasa vasorum profiles into the vessel wall of the thoracic aorta when compared with the abdominal aorta was clearly visible, even by microscopic examination (Fig. 7).

The complete data set with all the morphometric results for all of the samples of all aortic segments is provided in Appendix A.

4. Discussion

4.1. The tunica media of the thoracic aorta had a greater vasa vasorum density, and these vessels penetrated deeper into the aortic wall towards the lumen than in the abdominal aorta

The vasa vasorum density within the media decreased in the proximodistal direction (Fig. 2A), but the overall vasa vasorum density calculated per whole vessel wall showed greater values in the abdominal aorta than in the thoracic aorta (Fig. 2E). This finding appears to be a contradiction, but it is most probably the numerical result of a much thinner aortic media and whole wall in the abdominal segments (Fig. 2F in Tonar et al., 2015b). The reference area of the whole vascular wall section increases with the second power of the wall thickness, and therefore, the section area used as the denominator of the Q_A parameter is relatively greater in the thicker thoracic segments but relatively smaller in the thinner abdominal segments. Nevertheless, the greatest vasa vasorum density in the media found in the thoracic aorta suggests that the highly elastic thoracic segments require an especially rich microvessel network and that the thicker thoracic segments receive less direct diffusional support (Werber et al., 1987) from the lumen than the thinner distal segments do. The greater vasa vasorum density in the media3 sublayer than in the deeper (more abluminal) media4 to media5 sublayers in the thoracic aorta (Fig. 3A) suggests that another branching is generated in approximately the middle thickness of the media of the thoracic aorta.

Moreover, lower vasa vasorum densities within the media of the abdominal aorta might partially explain the vulnerability of the abdominal aorta to atherosclerosis or aneurysm formation (Heistad and Marcus, 1979). The precise role of the vasa vasorum in the mechanobiological stability (Humphrey and Holzapfel, 2012; Cyron and Humphrey, 2014a) and the propensity of the abdominal aorta to aneurysm formation (Cyron et al., 2014b) remains unclear. It is not known, whether the vasa vasorum morphology and penetration depth is linked to aortic remodelling and aneurysms formation due to the imbalance between the matrix metalloproteinases and their inhibitors (Sokolis and Iliopoulos, 2014).

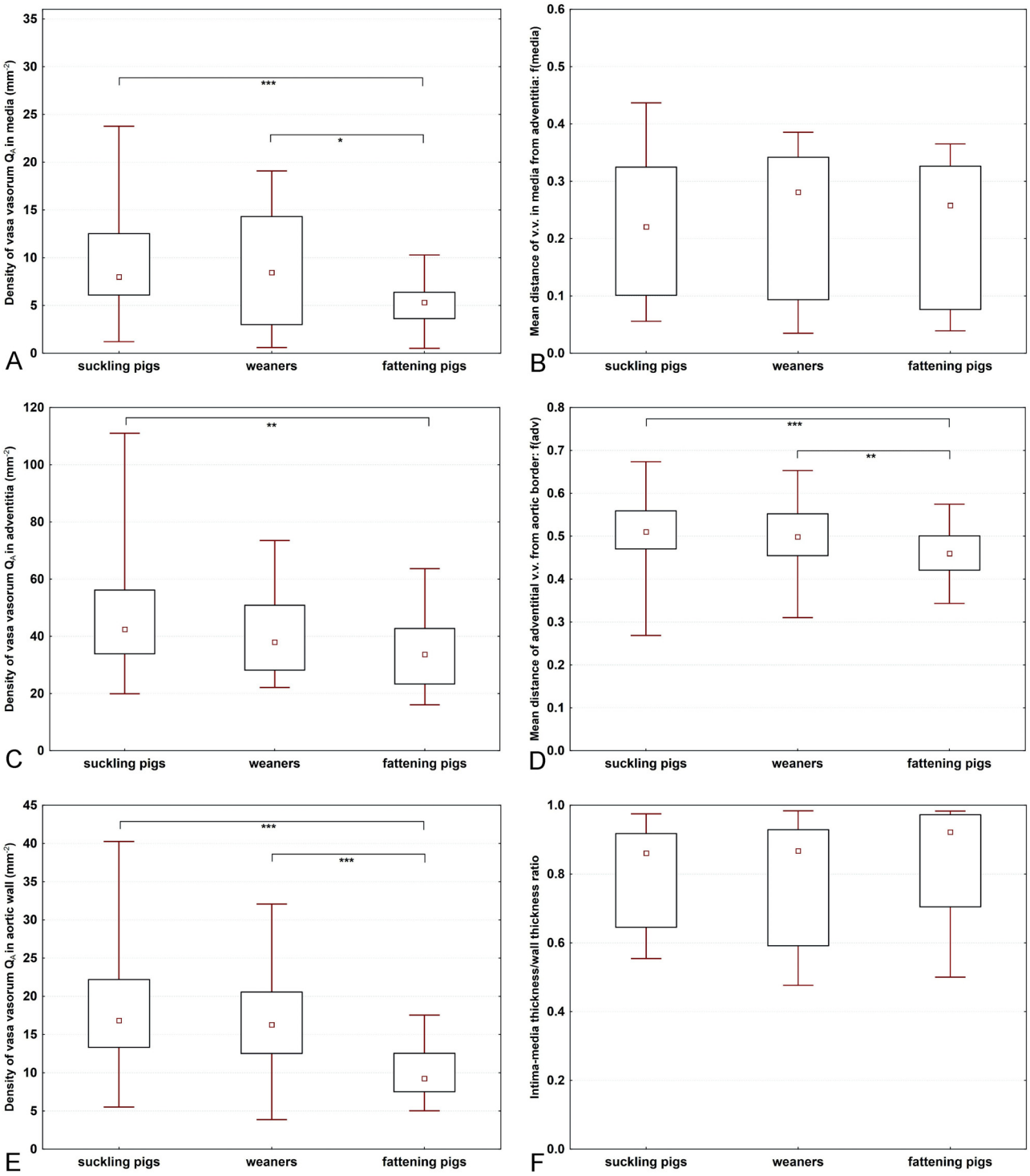

Fig. 4. Density of vasa vasorum (v.v.) profiles (Q_A) in the tunica media (A), the adventitia (C), and the aortic wall (E), together with the relative position of vasa vasorum profiles within the media (B) and adventitia (D) and the ratio of the intima-media thickness to the whole-wall thickness (F) in the three age groups of pigs. Aortic segments were pooled for this comparison. The differences between the age groups were first tested using the Kruskal–Wallis ANOVA test, which showed significant differences in the parameters shown under A ($p = 0.001$), C ($p = 0.02$), D ($p = 0.003$), and E ($p < 0.001$). For these parameters, the age groups were compared using the Mann–Whitney test (significant p-values are presented within the diagrams: $^{*}\ p < 0.05$, $^{**}\ p < 0.01$, $^{***}\ p < 0.001$). The data are displayed as the median values, with boxes spanning the upper limits of the first and third quartiles and with whiskers spanning the minimum and maximum values for each group.

Morphologically, the tunica adventitia proved to be a highly variable layer with respect to the aortic segments. In the proximodistal direction, the tunica adventitia is surrounded by a variety of tissues and microanatomical structures; i.e., a serous pericardial cavity, the loose connective tissue of the mediastinum and retroperitoneal fat, accompanied by a variable number of lymph nodes, aortic branches, and other structures. Surprisingly, this high level of anatomical variability did not affect the vasa vasorum density and distribution within the adventitia.

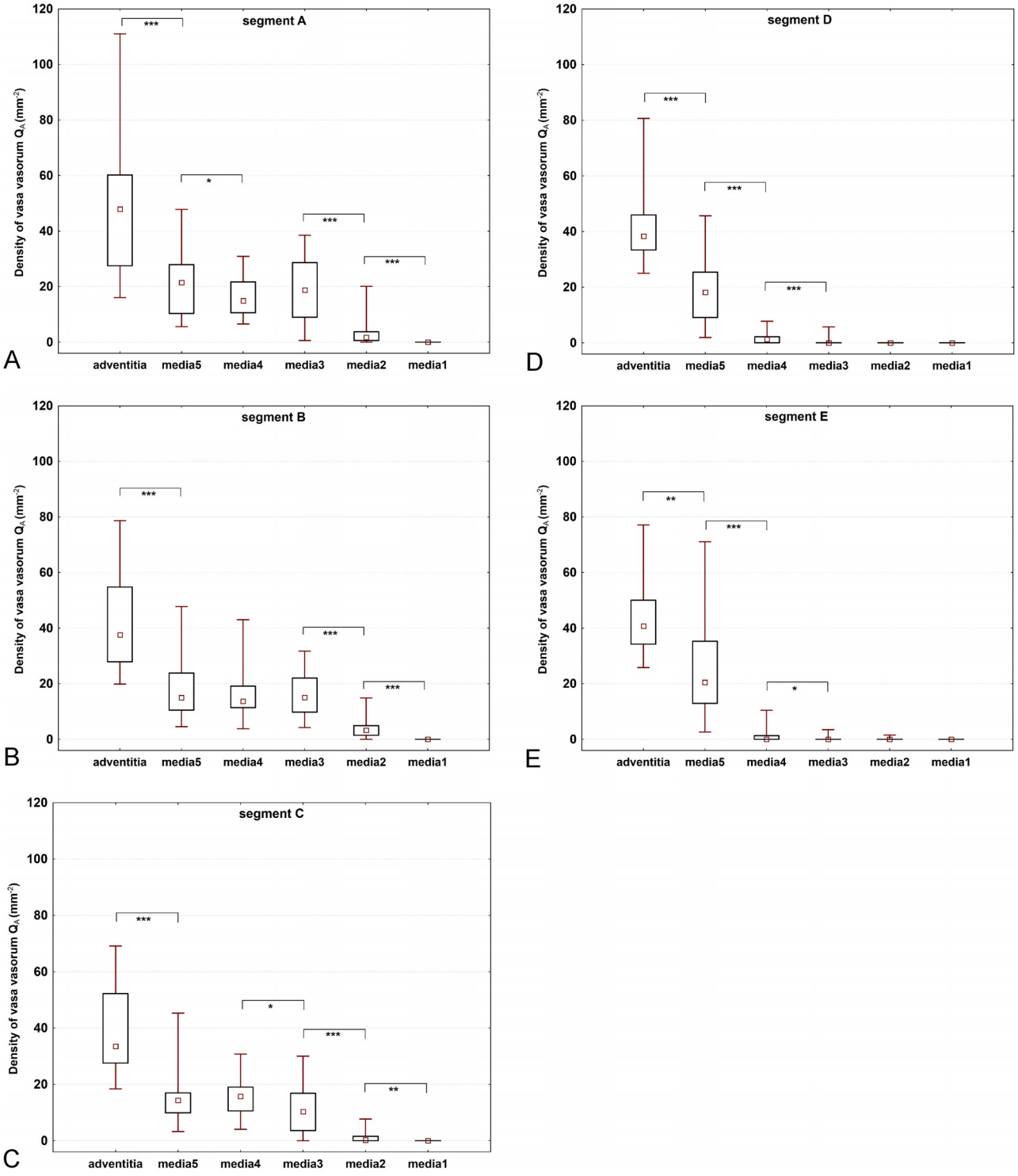

Fig. 5. Density of vasa vasorum profiles (Q_A) in the tunica adventitia and in the five virtual tunica media sublayers in the five proximodistal segments of the porcine thoracic (segments A–C in images A–C) and abdominal aorta (segments D–E in images D–E). For this comparison, the age groups were pooled, and the data from the corresponding images, sections and animals were exactly matched. The differences between layers were first tested using the Friedman ANOVA test, which showed significant differences in all segments ($p < 0.001$). Further comparisons between anatomically adjacent layers were performed using the Wilcoxon matched-pairs test (significant results are presented within the diagrams: * $p < 0.05$, ** $p < 0.01$, *** $p < 0.001$). In all segments, the adventitia had the greatest density of vasa vasorum profiles, followed by the most abluminal sublayer of the media (media5). The density of vasa vasorum gradually decreased towards the adluminal sublayers of the media until it reached zero in the innermost layer (media1) in the thoracic segments (A–C) or in the two innermost layers (media2 to media1) in the abdominal segments. Whereas the thoracic aorta (A–C) contained vasa vasorum profiles even within the middle medial sublayers (media3, i.e., 40–60% of the media thickness measured from the intima), these layers were avascular in the abdominal aortic segments (D–E). The data are displayed as the median values, with boxes spanning the upper limits of the first and third quartiles and with whiskers spanning the minimum and maximum values for each group.

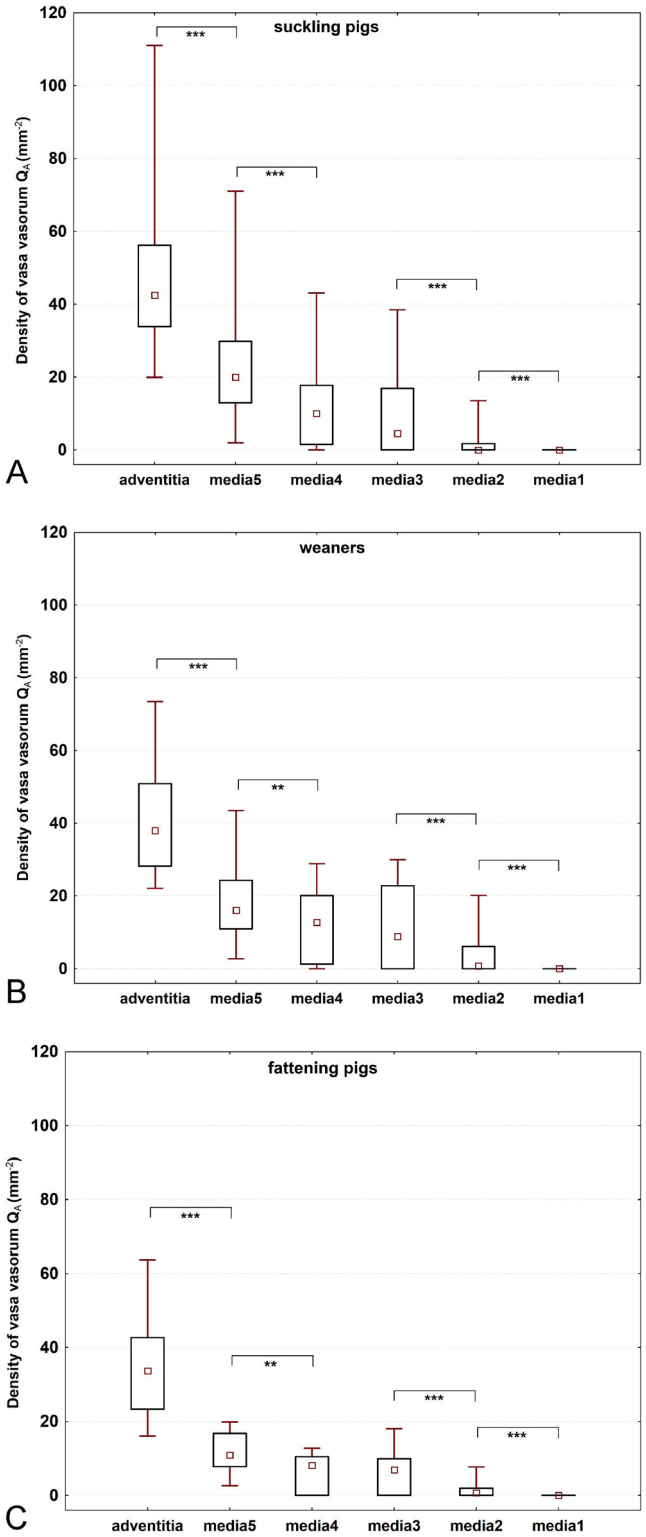

Fig. 6. Density of vasa vasorum profiles (Q_A) in the tunica adventitia and in the five tunica media sublayers in the three age groups of pigs: (A) suckling pigs, (B) weaners, and (C) fattening pigs. For this comparison, the aortic segments were pooled, and the data from the corresponding images, sections and animals were exactly matched. The differences between the layers were first tested using the Friedman ANOVA test, which showed significant differences in all age groups ($p < 0.001$). Further comparisons between anatomically adjacent layers were performed using the Wilcoxon matched-pairs test (significant results are presented within the diagrams: * $p < 0.05$, ** $p < 0.01$, *** $p < 0.001$). In all age groups, the adventitia had the greatest density of vasa vasorum profiles, followed by the most abluminal sublayer of the media (media5). No differences were found between the media3 and the media4 sublayers in any group, i.e., the density of profiles was the same within the middle region of the media (40–80% of the media thickness measured from the intima). The data are displayed as the median values, with boxes spanning the upper limits of the first and third quartiles and with whiskers spanning the minimum and maximum values for each group.

Table 2
Spearman rank-order correlations between the quantitative parameters.

	f (media)	Int + media thickness (IMT)	Q_A (adv.)	f (adv.)	Adventitia thickness (AT)	Q_A(wall)	Wall thickness (WT)	IMT/WT ratio	A_A (elastin)	A_A (collagen)	A_A (actin)	A_A (desmin)	A_A (vimentin)
Q_A(media)	0.56*	0.33*	–	–	−0.52*	–	–	0.49*	0.51*	–	−0.44*	−0.54*	–
f(media)	–	0.72*	–	–	−0.68*	−0.41*	0.55*	0.76*	0.67*	0.18*	−0.70*	−0.63*	−0.48*
Int + media thickness (IMT)	–	–	–	−0.26*	−0.48*	−0.63*	0.95*	0.80*	0.42*	0.32*	−0.63*	−0.39*	−0.63*
Q_A(adv.)	–	–	–	–	−0.19*	0.45*	−0.22*	–	–	−0.18*	–	–	–
f(adv.)	–	–	–	–	–	0.25*	−0.30*	–	–	–	–	–	0.25*
Adventitia thickness (AT)	–	–	–	–	–	0.35*	−0.24*	−0.88*	−0.67*	–	0.60*	0.56*	0.29*
Q_A(wall)	–	–	–	–	–	–	−0.60*	−0.56*	−0.31*	−0.21*	0.46*	0.24*	0.45*
Wall thickness (WT = IMT + AT)	–	–	–	–	–	–	–	0.61*	0.27*	0.30*	−0.49*	−0.21*	−0.61*
IMT/WT ratio	–	–	–	–	–	–	–	–	0.61*	–	−0.67*	−0.56*	−0.48*

Q_A(media)—density of vasa vasorum profiles within the intima and media; f(media)—mean distance of vasa vasorum profiles in the media from the adventitia; Int + media thickness (IMT)—total thickness of the intima and media; Q_A(adv.)—density of vasa vasorum profiles within the adventitia; f(adv.)—mean distance of vasa vasorum profiles in the adventitia from the outer border of the aortic wall; adventitia thickness (AT)—thickness of the adventitia; Q_A(wall)—density of vasa vasorum profiles per area unit of the whole section of the aortic wall; Wall thickness (WT) = IMT + AT. A_A *(elastin, collagen, actin, desmin, vimentin) indicates the area fraction of the respective component within the tunica intima and media reference areas. The values of the area fractions were taken from results previously published for the same tissue samples (Tonar et al., 2015b). For correlations between aortic wall constituents, see Tonar et al. (2015b).* The data were pooled across the experimental groups. Autocorrelations, repeating values and non-significant correlations have been replaced by the "–" sign.

* Indicates all correlations significant at $p < 0.05$.

4.2. The density of vasa vasorum gradually decreased with age in both the media and the adventitia

Vasa vasorum seemed to grow and branch less than necessary to maintain the same density of the microvascular bed within the aortic wall during growth and ageing (Fig. 4A and C). Interestingly, the relative position of vasa vasorum remained constant during ageing in most of the media (Fig. 4B), except the most abluminal fifth (Fig. 3B), but it was shifted outwards in the adventitia (Fig. 4D). This finding suggests that the depth into which vasa vasorum penetrate and where they branch remain proportional during the growth of the media. This phenomenon corresponds well with the relative proportions between the media and the adventitia, which remained constant during ageing as well (Fig. 4F). The aortic segments tend to retain their relative proportions of media thickness during growth, and the media of older animals receives less but equally distributed vasa vasorum. Although the absolute values of the media thickness increase significantly with age (Fig. 3F in Tonar et al., 2015b), the density of vasa vasorum does not differ between sucklings and weaners. This result can be regarded as indirect proof of vasa vasorum proliferation up to the weaners' age (29–75 days).

4.3. The adventitia contained more microvessels than the outer media did in all segments and age groups

Interpreting the greater density of vasa vasorum profiles in the adventitia when compared with the media (Figs. 5 and 6) is not entirely straightforward due to different histological compositions and presumably also to the differing metabolism of these layers. The adventitia of older animals had more vasa vasorum close to the adluminal border of the adventitia (Fig. 7). We believe that from these "near-media" adventitial vessels, branches enter the media, as suggested in a vasa vasorum analysis of the monkey aorta (Werber et al., 1987) and canine aorta (Stefanadis et al., 1995).

The completely avascular adluminal regions of the media in various proximodistal segments and age groups were mostly thinner than the approximate 0.5 mm value reported by Wolinsky and Glagov (1967, 1969) and Okuyama et al. (1988). This finding can be explained by the fact that appropriate immunohistochemical staining methods were not yet available in previous studies. Interestingly, the middle regions of the media comprising the 40–60% depth of the media thickness (measured from the intima) still contained non-negligible amounts of vasa vasorum profiles.

4.4. A thicker tunica media with higher elastin content correlated with greater density and deeper adluminal penetration of vasa vasorum

The number of significant correlations that we found (Table 2) demonstrates general mutual relations between the aortic wall microcirculation, the thickness, and aortic layer proportions. These relations are preserved beyond any biological interindividual variability or variability between the proximodistal segments and between age groups within the range of 0–230 days.

A greater density of the microvascular network in the media was significantly linked to deeper adluminal penetration. The vasa vasorum density within the media increased in aortic samples with relatively thicker media and thinner adventitia. This phenomenon was probably caused by extensive branching of the vasa vasorum within the media in proximal segments (see Section 4.3), where the adventitia was particularly thin and the media was comparatively thick. When the branching of the vasa vasorum was shifted into deeper layers, i.e., into the media and more close to the lumen, it appeared as an increased number of microvessel profiles with a greater probability of being sectioned and counted, and therefore, a greater microvessel density was observed.

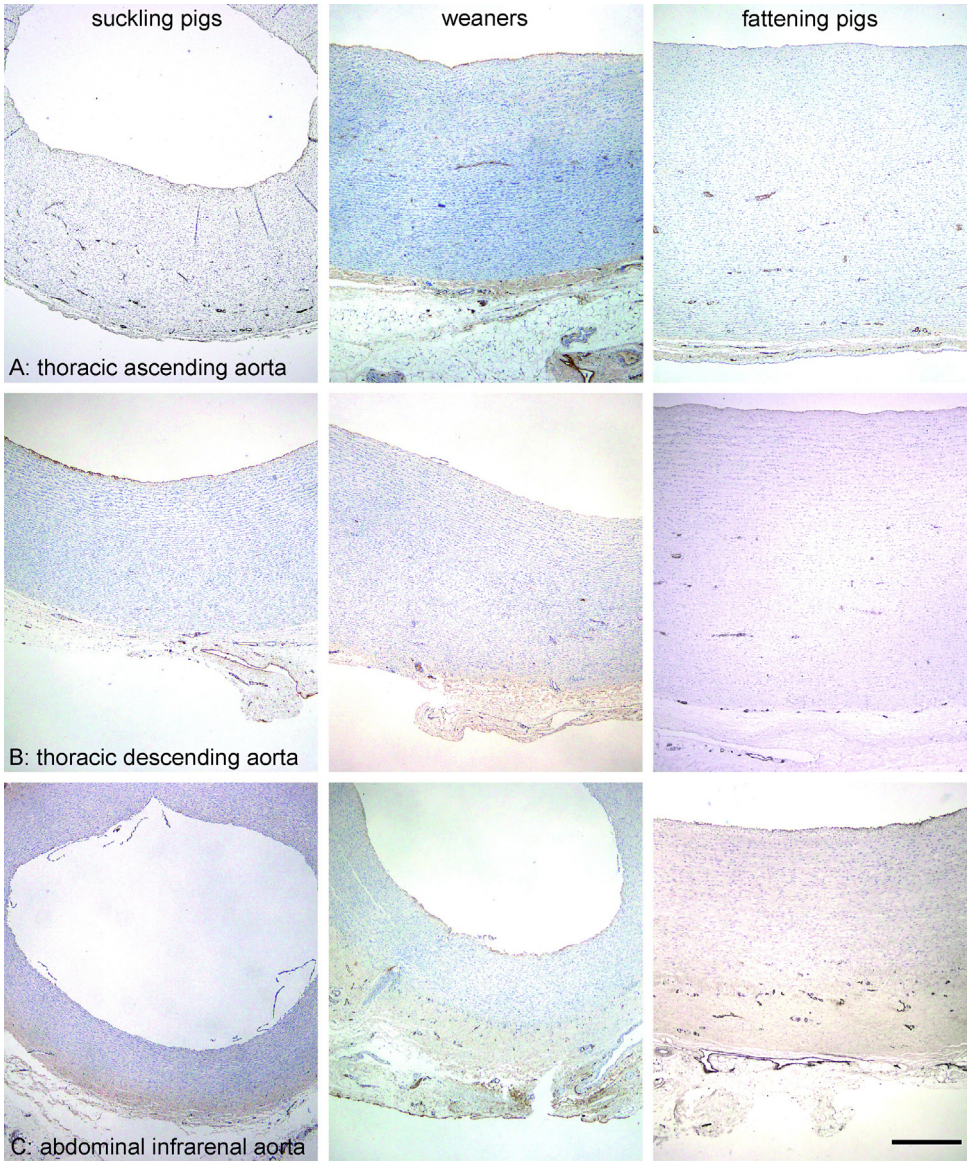

Fig. 7. Vasa vasorum within the thoracic ascending aorta (A), thoracic descending aorta (B), and infrarenal abdominal aorta (C) of suckling piglets (left), weaners (middle), and fattening pigs (right). The vasa vasorum density was highest in suckling pigs in both the media and the adventitia, and it gradually decreased with age. The relative position of the vasa vasorum within the media did not change with age, but older animals had more adventitial vasa vasorum close to the adluminal border of the adventitia. The relative media and adventitia thicknesses were retained during ageing in the corresponding aortic segments, although the overall thickness of the aortic wall increased. The density of the vasa vasorum in the media, but not in the adventitia, decreased in the proximodistal direction. In the thoracic aortic segments (A–B), the vasa vasorum penetrated deeper into the tunica media than in the abdominal aorta (C). In the thoracic aorta (A–B), the adventitia was thinner than in the abdominal aorta (C). Immunohistochemical detection of endothelial von Willebrand factor, visualization with horseradish peroxidase/diaminobenzidine (brown), counterstaining with haematoxylin. Scale bar: 500 μm (For interpretation of the references to color in this figure legend, the reader is referred to the web version of this article).

Segments with a greater elastin fraction within the media also had a greater density of vasa vasorum in the media. This result might be partially explained by the fact that an elastin network with transversally oriented elastic lamellae facilitates diffusion along the lamellae but restrains the diffusion of large molecules (such as albumin) across the media due to binding to these molecules (Hwang and Edelman, 2002; Goriely et al., 2007). Thus, segments with a rich elastin network can be expected to require an especially rich vascular network in the media, even though these segments have a smaller fraction of vascular smooth muscle cells at the same time. Conversely, the segments that contained relatively more vascular smooth muscle cells than elastin (mainly the abdominal segments, cf. Tonar et al., 2015b) had relatively lower vasa vasorum densities in the media and the microvessels did not penetrate too deeply (Table 2). Okuyama et al. (1988) suggested that the relatively greater vasa vasorum density in suckling piglets may be explained as the persistence of a prenatal rich vascular bed, which was interpreted as an adaptation to intrauterine hypoxia. However, this hypothesis was never confirmed.

4.5. Study implications

The adventitia thickness observed in the various segments under study was extremely variable, depending on both the proximodistal positions of the segments and anatomical directions; i.e., the adventitial structure and thickness lacked rotational symmetry. Moreover, it seems that two different layers of connective tissue outside the tunica media could be found: (i) a more adluminal layer of dense connective tissue that was unambiguously a part of the vessel wall and (ii) a more abluminal layer of loose connective

tissue often containing large numbers of fat cells. The latter was not considered as a part of the adventitia for the purposes of our study because it often contained preparation and dissection artefacts (namely microcracks), variable amounts of lymphatic tissue, and therefore, the vasa vasorum density would have been biased. However, this layer deserves a comparative anatomical study involving more animal species to clarify the general definition of the aortic adventitia.

Detailed mapping of vasa vasorum, including the segmental and age-related biological variability of the porcine aorta, is useful for understanding the drug distribution from arterial stents with fine control of locally directed drug release (Hwang and Edelman, 2002; Kusanagi et al., 2007), aortic implantation of mesenchymal stem cells in porcine models of aneurysm (Turnbull et al., 2011), or in hypercholesteroleamic pigs used as models in atherosclerosis research (Porras et al., 2015; Xu et al., 2015). Additionally, other experiments using a growing porcine model might benefit from the method and the data provided by the present study when evaluating aortic reconstruction and aortic arch replacement (Ioannou et al., 2003; Chen et al., 2012) or postoperative aortic compliance (Ioannou et al., 2013). For this purpose, the growth of the aortic wall may be described using the growth curves according to Gielecki et al. (2006) or Szpinda (2007). Analysis of vasa vasorum penetration would be useful also in tissue-engineered neovessels using polymeric scaffold matrices for developing biocompatible vascular grafts (Udelsman et al., 2014; Miller et al., 2015). In our opinion, future studies on vasa vasorum would highly benefit from using stereological morphometric parameters related to the vasculature, as recently summarized by Mühlfeld (2014).

The data provided in Appendix A can be directly used in modelling the spatial distribution of vasa vasorum using the stochastic geometry of point processes. This statistical technique already has many applications in quantitative description of geometrical structures in biology, medicine, and other research areas (for review, see Stoyan et al., 1995). For this purpose, the cross-sectional profiles of the originally three-dimensional microvessels appear as points, as usual in histological sections. Public-domain software is available (Baddeley and Turner, 2005; Baddeley et al., 2015) for modelling and analysing point patterns in two-, three-, or multidimensional space-time, which would be helpful when modelling the growth of vasa vasorum during ageing.

4.6. Study limitations and remarks on methods

Vasa vasorum represent a three-dimensional branching network, but the present study was based on their two-dimensional projections into a standardized transverse sectional plane. Analysis of prevailing directions (anisotropy) would require a three-dimensional approach (see Kochová et al. (2011) for current methods on the anisotropy of microvessels in histology), or at least a comparison of vasa vasorum profiles in multiple sectional planes (Tonar et al., 2012). By comparing longitudinal vs. transversal aortic sections, branching patterns of aortic vasa vasorum could be revealed in further studies, because more longitudinal first-order vasa have more probability to be sectioned by the transversal plane, whereas more circumferential second-order branches would appear more frequently on longitudinal sections. Another advance in quantifying vasa vasorum density would be using the orientator technique (Mattfeldt et al., 1990) to produce isotropic uniform random (IUR) sections, in which an unbiased length density L_V can be calculated from the two-dimensional density of vasa vasorum profiles Q_A using the simple formula $L_V = 2Q_A$. However, we did not select this IUR design, because analysis of media sublayers (hypotheses $H_0(A)$ and $H_0(C)$) relied on transversal sections; therefore, three-dimensional density of microvessels may not be calculated from our present results (Mühlfeld and Ochs, 2014).

Our vasa vasorum quantification did not differentiate the calibre of the vessels or whether they belonged to the arterial or venous part of the aortic microvascular bed. However, a reliable estimation of microvessel lumina in histological sections is difficult because the volume of, e.g., vasa vasorum is often collapsed in routinely processed histological samples. Volume collapse may be avoided by using perfusion fixation, which was not available during the collection of our samples. However, non-standard perfusion might introduce other artefacts into the preparations, such as overdistension or irregular distension of the vessels due to different wall properties.

Other study limitations are the same as in the previous paper on the same aortic segments (Tonar et al., 2015b), namely (i) the wall thickness measurements were affected by dissection of the aortae and by the *post mortem* contraction of the vascular segments, and no correction for the tissue shrinkage was performed; (ii) the study did not differentiate samples from the dorsal, lateral, and ventral sides of the abdominal aorta; (iii) the estimates were always based on one section per staining and anatomical position; and (iv) due to the number of animals, we did not perform simultaneous statistical analyses with grouping of the samples according to the aortic segments and age. Moreover, this morphological study does not offer information on the real perfusion rates of the aortic segments, as it is known that vasa vasorum are highly reactive and that their tone is physiologically regulated by a number of endogenous factors (Scotland et al., 2000).

4.7. Comparing porcine vs. human aortic vasa vasorum

Despite a thorough literature search, the information on human aortic vasa vasorum and their development are extremely rare. In our opinion, the results of the present study may not be extrapolated to the human aorta. Histological studies on age-dependent changes of human aortic vasa vasorum are lacking. Arteriolar and venous vasa vasorum of the ascending aorta, aortic arch, and descending aorta were examined in human between birth and 15 years of age using X-ray microscopy (Clarke, 1965), but the resolution limit of this radiological study was approximately 40 μm in diameter and most of the precapillary, capillary, and postcapillary vasa vasorum were missing in the study. Similarly to our study, Clarke (1965) proved that in human, the ascending aorta and aortic arch had a greater vasa vasorum density in neonates than at the end of the first year. Interestingly, the reverse was true for the descending thoracic and abdominal aorta. In human, Clarke (1965) reported a greater density of vasa vasorum arterioles and venules in the human abdominal than in the thoracic aorta, but the study did not detect the capillaries, which represent the most numerous population of the vasa vasorum in our immunohistochemical study. Moreover, statistical connections to the local wall thickness and histological composition of aortic wall (collagen, elastin, and smooth muscle fractions) in human ontogenesis are lacking. Increased knowledge on human aortic vasa vasorum would also be beneficial to transplantation medicine, because the external vascular supply of aortic branches originates from aortic vasa vasorum. This is important, e.g., for anastomosis of renal arteries during kidney transplantations (Kurzidim et al., 1999).

Studies mapping any age-related differences between these two species are missing. Despite many similarities between the porcine and human histology, such as diameter, thickness, and numbers of lamellar units (Wolinsky and Glagov, 1967), the results of the present study should be used in porcine models only and may not be easily extrapolated to the human aorta for several reasons. Major arteries (and also veins) contributed to the reorganization of the orthodynamics as a part of adaptations to the human upright gait (bipedism). Development of bipedal posture caused changes in pressure gradients, which required further changes in aortic

compliance when compared to quadrupeds. While the blood flow within the proximal part of the human aortic arch is under contraposition of gravity, the blood flow in the descending aorta goes along with the gravitational force vector. These differences may be measured when comparing the human vs. quadrupeds pulse wave velocity between carotid and femoral arteries (Neto, 2006). Moreover, hemodynamic responses to the orthostatic stress in human are modulated by the systolic volume ejection fraction, baroreflex sensitivity, activation of the renin–angiotensin–aldosterone system, renal sodium and water retention, systolic volume, and other cardiovascular adaptations, in which differences are found between quadrupeds and human (Neto, 2006). In addition, differences in aortic gross anatomy and histology are to be taken into account, such as variations in branching aortic patterns (especially in the aortic arch), and various amounts of periaortic connective tissue and anatomical relations between descending aorta to the vertebral bodies.

5. Conclusion

We estimated the density of von Willebrand factor-positive profiles of vasa vasorum per profile area of the aortic wall using transversal histological sections in five proximodistal segments sampled from the porcine aortae of growing pigs of age ranging from 0 to 230 days. The tunica media of the thoracic aorta had a greater vasa vasorum density, with microvessels penetrating deeper towards the lumen than in the abdominal aorta. The density of vasa vasorum gradually decreased with age in both the media and the adventitia. The depth into which vasa vasorum penetrated and where they branched remained proportional during the ageing and growth of the media. The aortic segments retained their relative proportions between the media thickness and the adventitia thickness during growth, and the media of older animals received less but equally distributed vasa vasorum. A greater density of vasa vasorum in the media was significantly linked to greater media thickness and a greater elastin fraction (data on elastin taken from another study on the same samples). The immunohistochemical quantification revealed deeper penetration of vasa vasorum into the tunica media, reaching adluminal layers of the vessel wall that were hitherto reported to be avascular. The complete primary morphometric data in the form of continuous variables have been made available as a supplement to this paper. Mapping of the vasa vasorum profiles density and position has promising illustrative potential for studies on the aorta in experimental porcine models, such as models of atherosclerotic and inflammatory neovascularization, aortic aneurysms and drug distribution from arterial stents.

Acknowledgements

This study was supported by the National Sustainability Program I (NPU I) Nr. LO1503 provided by the Ministry of Education, Youth and Sports of the Czech Republic and by the Prvouk P36 Project of the Charles University in Prague. This study was also partially supported by Ministry of Health of the Czech Republic, Project Nr. AZV 15-32727A. Skilful technical support from Ms. Magdalena Helmreich, Ms. Anne Flemming, Ms. Claudia Höchsmann and Ms. Brigitte Machac is gratefully acknowledged.

Appendix A. Supplementary data

Supplementary data associated with this article can be found, in the online version, at http://dx.doi.org/10.1016/j.aanat.2016.01.008.

References

Aguirre-Sanceledonio, M., Fossum, T.W., Miller, M.W., Humphrey, J.D., Berridge, B.R., Herráez, P., 2003. Collateral circulation in experimental coarctation of the aorta in minipigs: a possible association with hypertrophied vasa vasorum. J. Comp. Pathol. 128, 165–171.

Angouras, D., Sokolis, D.P., Dosios, T., Kostomitsopoulos, N., Boudoulas, H., Skalkeas, G., Karayannacos, P.E., 2000. Effect of impaired vasa vasorum flow on the structure and mechanics of the thoracic aorta: implications for the pathogenesis of aortic dissection. Eur. J. Cardiothorac. Surg. 17, 468–473.

Baddeley, A., Turner, R., 2005. Spatstat: an R package for analyzing spatial point patterns. J. Stat. Softw. 12, 1–42.

Baddeley, A., Rubak, E., Turner, R., 2015. Spatial Point Patterns: Methodology and Applications with R. Chapman and Hall/CRC Press, London.

Baikoussis, N.G., Apostolakis, E.E., Papakonstantinou, N.A., Siminelakis, S.N., Arnaoutoglou, H., Papadopoulos, G., Goudevenos, J., Dougenis, D., 2011. The implication of vasa vasorum in surgical diseases of the aorta. Eur. J. Cardiothorac. Surg. 40, 412–417.

Chen, C.C., Tseng, Y.C., Lin, C.C., Li, C.F., Yeh, M.L., 2012. A modular branched stent-graft system for sutureless anastomoses in extensive aortic arch replacement—a porcine study. Ann. Vasc. Surg. 26, 527–536.

Clarke, J.A., 1965. An x-ray microscopic study of the postnatal development of the vasa vasorum in the human aorta. J. Anat. 99, 877–889.

Cyron, C.J., Humphrey, J.D., 2014a. Vascular homeostasis and the concept of mechanobiological stability. Int. J. Eng. Sci. 85, 203–223.

Cyron, C.J., Wilson, J.S., Humphrey, J.D., 2014b. Mechanobiological stability: a new paradigm to understand the enlargement of aneurysms? J. R. Soc. Interface 11, 20140680.

Desai, M., Ahmed, M., Darbyshire, A., You, Z., Hamilton, G., Seifalian, A.M., 2011. An aortic model for the physiological assessment of endovascular stent-grafts. Ann. Vasc. Surg. 25, 530–537.

Dziodzio, T., Juraszek, A., Reineke, D., Jenni, H., Zermatten, E., Zimpfer, D., Stoiber, M., Scheikl, V., Schima, H., Grimm, M., Czerny, M., 2011. Experimental acute type B aortic dissection: different sites of primary entry tears cause different ways of propagation. Ann. Thorac. Surg. 91, 724–727.

Eberlova, L., Tonar, Z., Witter, K., Krizkova, V., Nedorost, L., Korabecna, M., Tolinger, P., Kocova, J., Boudova, L., Treska, V., Houdek, K., Molacek, J., Vrzalova, J., Pesta, M., Topolcan, O., Valenta, J., 2013. Asymptomatic abdominal aortic aneurysms show histological signs of progression: a quantitative histochemical analysis. Pathobiology 80, 11–23.

Fleiner, M., Kummer, M., Mirlacher, M., Sauter, G., Cathomas, G., Krapf, R., Biedermann, B.C., 2004. Arterial neovascularization and inflammation in vulnerable patients: early and late signs of symptomatic atherosclerosis. Circulation 110, 2843–2850.

Funder, J.A., Frost, M.W., Klaaborg, K.E., Wierup, P., Hjortdal, V., Nygaard, H., Hasenkam, J.M., 2012. Aortic root distensibility after subcoronary stentless valve implantation. J. Heart Valve Dis. 21, 181–188.

Gabner, S., Tonar, Z., Tichy, A., Saalmüller, A., Worliczek, H.L., Joachim, A., Witter, K., 2012. Immunohistochemical detection and quantification of T cells in the small intestine of *Isospora suis*-infected piglets—influence of fixation technique and intestinal segment. Microsc. Res. Tech. 75, 408–415.

Galili, O., Herrmann, J., Woodrum, J., Sattler, K.J., Lerman, L.O., Lerman, A., 2004. Adventitial vasa vasorum heterogeneity among different vascular beds. J. Vasc. Surg. 40, 529–535.

Gielecki, J.S., Syc, B., Wilk, R., Musiał-Kopiejka, M., Piwowarczyk-Nowak, A., 2006. Quantitative evaluation of aortic arch development using digital-image analysis. Ann. Anat. 188, 19–23.

Goriely, A.R., Baldwin, A.L., Secomb, T.W., 2007. Transient diffusion of albumin in aortic walls, effects of binding to medial elastin layers. Am. J. Physiol. Heart Circ. Physiol. 292, H2195–H2201.

Granada, J.F., Feinstein, S.B., 2008. Imaging of the vasa vasorum. Nat. Clin. Pract. Cardiovasc. Med. Suppl 2, S18–S25.

Gundersen, H.J., 1977. Notes on the estimation of the numerical density of arbitrary profiles: the edge effect. J. Microsc. 111, 219–223.

Heistad, D.D., Marcus, M.L., 1979. Role of vaso vasorum in nourishment of the aorta. Blood Vessel. 16 (5), 225–238.

Houdek, K., Moláček, J., Třeška, V., Křížková, V., Eberlová, L., Boudová, L., Nedorost, L., Tolinger, P., Kočová, J., Kobr, J., Baxa, J., Liška, V., Witter, K., Tonar, Z., 2013. Focal histopathological progression of porcine experimental abdominal aortic aneurysm is mitigated by atorvastatin. Int. Angiol. 32, 291–306.

Humphrey, J.D., Holzapfel, G.A., 2012. Mechanics, mechanobiology, and modeling of human abdominal aorta and aneurysms. J. Biomech. 45, 805–814.

Hwang, C.W., Edelman, E.R., 2002. Arterial ultrastructure influences transport of locally delivered drugs. Circ. Res. 90, 826–832.

Ioannou, C.V., Stergiopulos, N., Katsamouris, A.N., Startchik, I., Kalangos, A., Licker, M.J., Westerhof, N., Morel, D.R., 2003. Hemodynamics induced after acute reduction of proximal thoracic aorta compliance. Eur. J. Vasc. Endovasc. Surg. 26, 195–204.

Ioannou, C.V., Stergiopulos, N., Georgakarakos, E., Chatzimichali, E., Katsamouris, A.N., Morel, D.R., 2013. Effects of isoflurane anesthesia on aortic compliance and systemic hemodynamics in compliant and noncompliant aortas. J. Cardiothorac. Vasc. Anesth. 27, 1282–1288.

Johnson, J.J., Jacocks, M.A., Gauthier, S.C., Irwin, D.A., Wolf, R.F., Garwe, T., Lerner, M.R., Lees, J.S., 2013. Establishing a swine model to compare vascular prostheses in a contaminated field. J. Surg. Res. 181, 355–358.

Kim, J., Baek, S., 2011. Circumferential variations of mechanical behavior of the porcine thoracic aorta during the inflation test. J. Biomech. 44, 1941–1947.
Kochová, P., Cimrman, R., Janáček, J., Witter, K., Tonar, Z., 2011. How to asses, visualize and compare the anisotropy of linear structures reconstructed from optical sections—a study based on histopathological quantification of human brain microvessels. J. Theor. Biol. 286, 67–78.
Kocova, J., 1970. Overall staining of connective tissue and the muscular layer of vessels. Folia Morphol. 18, 293–295.
Kurzidim, M.H., Oeschger, M., Sasse, D., 1999. Studies on the vasa vasorum of the human renal artery. Ann. Anat. 181, 223–227.
Kusanagi, M., Matsui, O., Sanada, J., Ogi, T., Takamatsu, S., Zhong, H., Kimura, Y., Tabata, Y., 2007. Hydrogel-mediated release of basic fibroblast growth factor from a stent-graft accelerates biological fixation with the aortic wall in a porcine model. J. Endovasc. Ther. 14, 785–793.
Lillie, M.A., Armstrong, T.E., Gérard, S.G., Shadwick, R.E., Gosline, J.M., 2012. Contribution of elastin and collagen to the inflation response of the pig thoracic aorta: assessing elastin's role in mechanical homeostasis. J. Biomech. 45, 2133–2141.
Mattfeldt, T., Mall, G., Gharehbaghi, H., Moller, P., 1990. Estimation of surface area and length with the orientator. J. Microsc. 159, 301–317.
Miller, K.S., Khosravi, R., Breuer, C.K., Humphrey, J.D., 2015. A hypothesis-driven parametric study of effects of polymeric scaffold properties on tissue engineered neovessel formation. Acta Biomater. 11, 283–294.
Moreno, P.R., Purushothaman, K.R., Zias, E., Sanz, J., Fuster, V., 2006. Neovascularization in human atherosclerosis. Curr. Mol. Med. 6, 457–477.
Moulton, K.S., Vakili, K., Zurakowski, D., Soliman, M., Butterfield, C., Sylvin, E., Lo, K.M., Gillies, S., Javaherian, K., Folkman, J., 2003. Inhibition of plaque neovascularization reduces macrophage accumulation and progression of advanced atherosclerosis. Proc. Natl. Acad. Sci. USA 100, 4736–4741.
Mühlfeld, C., 2014. Quantitative morphology of the vascularisation of organs: a stereological approach illustrated using the cardiac circulation. Ann. Anat. 196, 12–19.
Mühlfeld, C., Ochs, M., 2014. Measuring structure—what's the point in counting? Ann. Anat. 196, 1–2.
Nedorost, L., Uemura, H., Furck, A., Saeed, I., Slavik, Z., Kobr, J., Tonar, Z., 2013. Vascular histopathologic reaction to pulmonary artery banding in an in vivo growing porcine model. Pediatr. Cardiol. 34, 1652–1660.
Neto, E., 2006. Great arteries contribution in orthostasis cardiovascular adaptation. Arq. Bras. Cardiol. 87, 209–222.
Newby, A.C., Zaltsman, A.B., 2000. Molecular mechanisms in intimal hyperplasia. J. Pathol. 190, 300–309.
Nickel, R., Schummer, A., Seiferle, E., 1996. Lehrbuch der Anatomie der Haustiere. Band III Kreislaufsystem, Haut und Hautorgane, third ed. Parey Buchverlag, Berlin.
Okuyama, K., Yaginuma, G., Takahashi, T., Sasaki, H., Mori, S., 1988. The development of vasa vasorum of the human aorta in various conditions. A morphometric study. Arch. Pathol. Lab. Med. 112, 721–725.
Ondrovics, M., Silbermayr, K., Mitreva, M., Young, N.D., Razzazi-Fazeli, E., Gasser, R.B., Joachim, A., 2013. Proteomic analysis of *Oesophagostomum dentatum* (Nematoda) during larval transition, and the effects of hydrolase inhibitors on development. PLoS ONE 8, e63955.
Ordóñez, N.G., 2012. Immunohistochemical endothelial markers: a review. Adv. Anat. Pathol. 19, 281–295.
Porras, A.M., Shanmuganayagam, D., Meudt, J.J., Krueger, C.G., Hacker, T.A., Rahko, P.S., Reed, J.D., Masters, K.S., 2015. Development of aortic valve disease in familial hypercholesterolemic swine: implications for elucidating disease etiology. J. Am. Heart Assoc. 4, e002254.
Ritman, E.L., Lerman, A., 2007. The dynamic vasa vasorum. Cardiovasc. Res. 75, 649–658.
Romeis, B., 1989. Mikroskopische Technik. Urban & Schwarzenberg, München.
Saari, P., Lähteenvuo, M., Honkonen, K., Manninen, H., 2012. Antegrade in situ fenestration of aortic stent graft: in-vivo experiments using a pig model. Acta Radiol. 53, 754–758.
Sarda-Mantel, L., Alsac, J.M., Boisgard, R., Hervatin, F., Montravers, F., Tavitian, B., Michel, J.B., Le Guludec, D., 2012. Comparison of 18F-fluoro-deoxy-glucose, 18F-fluoro-methyl-choline, and 18F-DPA714 for positron-emission tomography imaging of leukocyte accumulation in the aortic wall of experimental abdominal aneurysms. J. Vasc. Surg. 56, 765–773.
Scotland, R.S., Vallance, P.J., Ahluwalia, A., 2000. Endogenous factors involved in regulation of tone of arterial vasa vasorum: implications for conduit vessel physiology. Cardiovasc. Res. 46, 403–411.
Shadwick, R.E., 1999. Mechanical design in arteries. J. Exp. Biol. 202, 3305–3313.
Sokolis, D.P., 2007. Passive mechanical properties and structure of the aorta: segmental analysis. Acta Physiol. (Oxf.) 190, 277–289.
Sokolis, D.P., Boudoulas, H., Karayannacos, P.E., 2008. Segmental differences of aortic function and composition: clinical implications. Hellenic J. Cardiol. 49, 145–154.
Sokolis, D.P., Iliopoulos, D.C., 2014. Impaired mechanics and matrix metalloproteinases/inhibitors expression in female ascending thoracic aortic aneurysms. J. Mech. Behav. Biomed. Mater. 34, 154–164.
Szpinda, M., 2007. Morphometric study of the ascending aorta in human fetuses. Ann. Anat. 189, 465–472.
Stefanadis, C., Vlachopoulos, C., Karayannacos, P., Boudoulas, H., Stratos, C., Filippides, T., Agapitos, M., Toutouzas, P., 1995. Effect of vasa vasorum flow on structure and function of the aorta in experimental animals. Circulation 91, 2669–2678.
Stoyan, D., Kendall, W.S., Mecke, J., 1995. Stochastic Geometry and its Applications, second ed. John Wiley & Sons, Chichester.
Tonar, Z., Kural Jr., T., Kochova, P., Nedorost, L., Witter, K., 2012. Vasa vasorum quantification in human varicose great and small saphenous veins. Ann. Anat. 194, 473–481.
Tonar, Z., Kochova, P., Cimrman, R., Perktold, J., Witter, K., 2015a. Segmental differences in the orientation of smooth muscle cells in the tunica media of porcine aortae. Biomech. Model. Mechanobiol. 14, 315–332.
Tonar, Z., Kubíková, T., Prior, C., Demjén, E., Liška, V., Králíčková, M., Witter, K., 2015b. Segmental and age differences in the elastin network, collagen, and smooth muscle phenotype in the tunica media of the porcine aorta. Ann. Anat. 201, 79–90.
Turnbull, I.C., Hadri, L., Rapti, K., Sadek, M., Liang, L., Shin, H.J., Costa, K.D., Marin, M.L., Hajjar, R.J., Faries, P.L., 2011. Aortic implantation of mesenchymal stem cells after aneurysm injury in a porcine model. J. Surg. Res. 170, e179–e188.
Udelsman, B.V., Khosravi, R., Miller, K.S., Dean, E.W., Bersi, M.R., Rocco, K., Yi, T., Humphrey, J.D., Breuer, C.K., 2014. Characterization of evolving biomechanical properties of tissue engineered vascular grafts in the arterial circulation. J. Biomech. 47, 2070–2079.
Werber, A.H., Armstrong, M.L., Heistad, D.D., 1987. Diffusional support of the thoracic aorta in atherosclerotic monkeys. Atherosclerosis 68, 123–130.
Witter, K., Tonar, Z., Matejka, V.M., Martinca, T., Jonak, M., Rokosny, S., Pirk, J., 2010. Tissue reaction to three different types of tissue glues in an experimental aorta dissection model: a quantitative approach. Histochem. Cell Biol. 133, 241–259.
Wolinsky, H., Glagov, S., 1967. Nature of species differences in the medial distribution of aortic vasa vasorum in mammals. Circ. Res. 20, 409–421.
Wolinsky, H., Glagov, S., 1969. Comparison of abdominal and thoracic aortic medial structure in mammals. Deviation of man from the usual pattern. Circ. Res. 25, 677–686.
Worliczek, H.L., Buggelsheim, M., Alexandrowicz, R., Witter, K., Schmidt, P., Gerner, W., Saalmüller, A., Joachim, A., 2010. Changes in lymphocyte populations in suckling piglets during primary infections with *Isospora suis*. Parasite Immunol. 32, 232–244.
Xu, X., Mao, W., Chai, Y., Dai, J., Chen, Q., Wang, L., Zhuang, Q., Pan, Y., Chen, M., Ni, G., Huang, Z., 2015. Angiogenesis inhibitor, endostar, prevents vasa vasorum neovascularization in a swine atherosclerosis model. J. Atheroscler. Thromb. 22, 1100–1112.